Flood, R.D., Piper, D.J.W., Klaus, A., and Peterson, L.C. (Eds.), 1997
Proceedings of the Ocean Drilling Program, Scientific Results, Vol. 155

3. GRAIN-SIZE CHARACTERIZATION OF AMAZON FAN DEPOSITS AND COMPARISON TO SEISMIC FACIES UNITS[1]

Patricia L. Manley,[2] Carlos Pirmez,[3] William Busch,[4] and Adrian Cramp[5]

ABSTRACT

Prior to Ocean Drilling Program Leg 155, the architecture of the Amazon Fan, as well as those of other modern submarine fans, had been investigated primarily by seismic reflection profiles. The acoustic facies and stratal patterns observed on these profiles provided a wealth of information that allowed deciphering fan growth patterns and the geometry of fan deposits. However, lithofacies could only be inferred from the seismic reflection data. Here we analyze grain-size data from 13 sites drilled during Leg 155, and place the results in the context of the stratigraphic units interpreted from seismic reflection data. Clay, silt, and fine sand are the dominant grain sizes of all cores retrieved from the Amazon Fan. In this mud-rich fan, sand is concentrated within the channel thalweg, at the base of channel-levee systems within the middle fan, and forms a significant fraction of the lower fan deposits drilled. All channel-levee deposits drilled are characterized by a fining-upward trend and by an overall coarsening in the downfan direction. Downfan coarsening of the levee deposits probably results from very efficient sorting associated with the channelized flow of turbidity currents together with the overall decrease in channel relief downfan. Fining-upward cycles within a channel-levee system are observed in the middle fan where multiple phases of levee development are stacked upon each other. Each growth phase is marked by an abrupt coarsening that marks a channel bifurcation occurring downslope, followed by a fining-upward sequence of levee aggradation. Channel bifurcation results in the reworking of older channel deposits, and the formation of laterally widespread units. High-amplitude reflections (HARs) beneath the channel axis and high-amplitude reflection packet (HARPs) units are composed of two distinct grain-size populations. HARs and HARPs are the coarsest units that form the fan, with sizes up to 0 ø. Both units display an overall coarsening downfan. These characteristics are likely the result of multistep transport of sand downfan. Thick acoustically transparent units on seismic profiles are correlated to large mass-transport deposits, displaying grain-size characteristics similar to levee deposits with an overall fining-upward and downfan-coarsening trend.

INTRODUCTION

Two major acoustic units alternate to build the fan, large levee complexes and mass-transport deposits (Figs. 1, 2). This cyclic pattern was recognized within the upper and middle Amazon Fan (Manley and Flood, 1988) and led to the identification of four stacked channel-levee complexes. The youngest, the Upper Levee Complex (ULC, isotope Stages 2–4), overlies both the Middle Levee Complex (MLC, isotope Stage 6) and the Lower Levee Complex (LLC, isotope Stage 8) while the Bottom Levee Complex (BLC) appears stratigraphically below all three (Flood et al., 1991; Flood, Piper, Klaus, et al., 1995) (Fig. 2). Interfingered with these complexes are mass-transport deposits (Table 1).

Each levee complex is built by individual channel-levee systems that overlap and coalesce. Channel-levee systems are large, acoustically semitransparent, lens-shaped overbank deposits with a distributary channel near the center. The channel axes are associated with high-amplitude reflections (HARs, Kastens and Shor, 1985) on seismic reflection profiles. The relative age relationships of the systems were determined for the surficial channels by overlapping stratigraphic relationships (named 1 through 6C; Damuth et al., 1983a, 1983b, 1988; Damuth and Flood, 1984), whereas the stratigraphy of buried channel-levee systems used overlapping stratigraphic relationships as well as depth to levee crests (given color names; Manley and Flood, 1988) (Table 1; Figs. 1, 2). The levee complex grows with repeated avulsions of older channels. At the location of an avulsion, a new channel-levee system begins to build on top of older channel-levee systems downfan (Figs. 2, 3). Within the middle fan, lobe-like, high-amplitude refection packets (HARPs) underlie the newly formed channel-levee systems and are related to the avulsion. These HARP units extend downfan from the point of bifurcation to form part of the lower fan (Flood et al., 1991). Thus, several seismic architectural units (e.g., channel-levee systems, mass-transport deposits, HARs, and HARPs) have been previously mapped throughout the Amazon Fan (Damuth et al., 1988; Manley and Flood, 1988; Flood et al., 1991; Pirmez, 1994; Pirmez and Flood, 1995). During ODP Leg 155, holes at 17 sites were drilled through these acoustically defined units, and approximately 4 km of Pleistocene-age sediment was recovered (Figs. 1, 2).

Limited grain-size studies have been done on sediments from modern fans, usually sampling only the upper 20 m via piston cores. Although two modern fans have been drilled, the Mississippi Fan (Deep Sea Drilling Project [DSDP] Leg 96) (Stow et al., 1985) and the distal portion of the Bengal Fan (ODP Leg 116) (Stow and Wetzel, 1990), no known studies have ever sampled the *same* acoustic units systematically from the upper to the lower fan.

Individual sites had specific drill objectives (Flood, Piper, Klaus, et al., 1995), but because of the previous seismic stratigraphic knowledge of the fan, several sites (specifically Sites 930, 935, 936, 939, 940, 943, 945, 944, 945, and 946) were drilled within the most recently active channel-levee system (named the Amazon system) of the ULC. These sites allowed for characterization of downfan variation in several acoustically identified units. In addition, some sites (Sites 931, 933, 935, 936, and 944) penetrated the stacked channel-levee complexes, allowing characterization of older channel-levee complexes (MLC, LLC, and BLC) (Fig. 2).

[1]Flood, R.D., Piper, D.J.W., Klaus, A., and Peterson, L.C. (Eds.), 1997. *Proc. ODP, Sci. Results*, 155: College Station, TX (Ocean Drilling Program).

[2]Geology Department, Middlebury College, Middlebury, VT 05753, U.S.A. patmanley@mail.middlebury.edu
[3]Lamont-Doherty Earth Observatory, Columbia University, Palisades, NY 10964, U.S.A.
[4]Department of Geology and Geophysics, University of New Orleans, New Orleans, LA 70148, U.S.A.
[5]Department of Geology, College of Cardiff, University of Wales, Cardiff CF1 3YE United Kingdom.

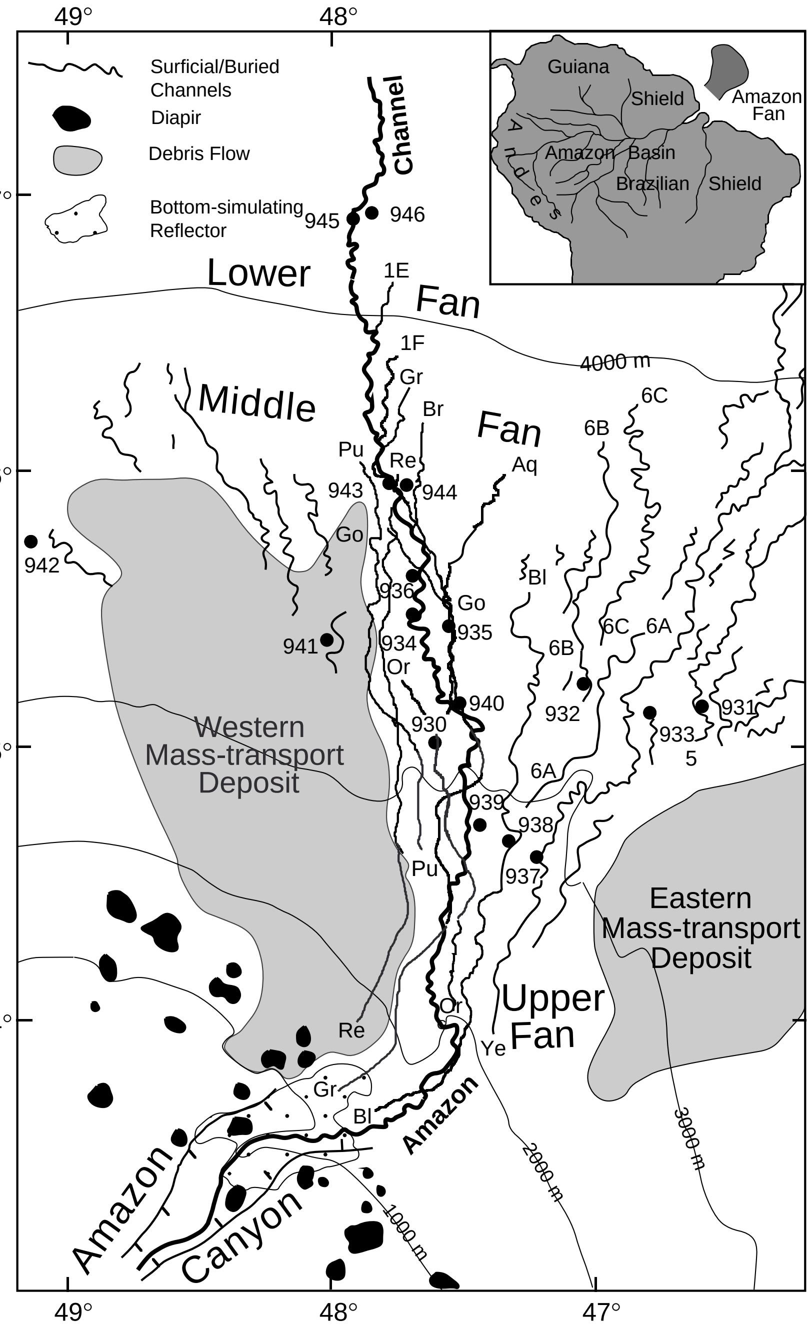

Figure 1. Generalized map of the Amazon Fan (after Flood, Piper, Klaus, et al., 1995). Site locations are shown relative to surficial and buried channel-levee systems and surface mass-transport deposits. Older channel-levee systems are labeled by letter or number using the nomenclature developed by Damuth et al., 1988, and Manley and Flood, 1988. Channel-levee systems Aqua (Aq), Brown (Br), 1E, and 1F are related to bifurcations associated with the development of the most recently active channel, Amazon Channel, on the Amazon Fan.

Grain-size analyses have been performed on sediment correlated to these acoustic units. By systematically determining the grain size of the sediments from the Amazon Fan, we can investigate several of the sedimentological processes that formed the fan. In addition, this can assist in our understanding of the spatial and temporal development of the Amazon deep-sea fan. Grain-size data and interpretation of the architectural units are presented in two parts: (1) the grain size for individual holes and (2) the depositional processes of the architectural units.

Material and Methods

Grain-size analysis was determined on physical property residues obtained during Leg 155. Physical properties samples taken on board (approximately 10 cm^3) were recovered from undisturbed core intervals and often were preferentially sampled avoiding the coarser silt/sand layers, which were commonly disturbed by drilling.

Sediment samples of approximately 1 g dry weight were prepared using 50 mL of dispersing solution (a solution of sodium hexametaphosphate [Calgon] and filtered water at a concentration of 38 g/L). To assist dissemination, the sediment was vigorously stirred with a soft bristled brush while in an ultrasound bath. Grain-size determination was performed using a Malvern MasterSizer E at Hamilton College (Clinton, New York). The Malvern MasterSizer E uses a laser-diffraction technique in order to determine particle size (McCave et al., 1986). Given that particles of a certain size diffract the laser beam at different angles, the machine can detect and differentiate those angles, providing a grain-size distribution. There is no bias based on grain shape or settling rate with the Malvern MasterSizer E. Because the sample is kept in suspension in a turbulent flow within the lens detector, this randomizes the orientation of the grain so all axes of the grain are used in the grain-size distribution analysis. For this study, a He-Ne laser, a poly-disperse model, and a 300-mm lens were used to enable detection with the greatest range (1.2–600 µm).

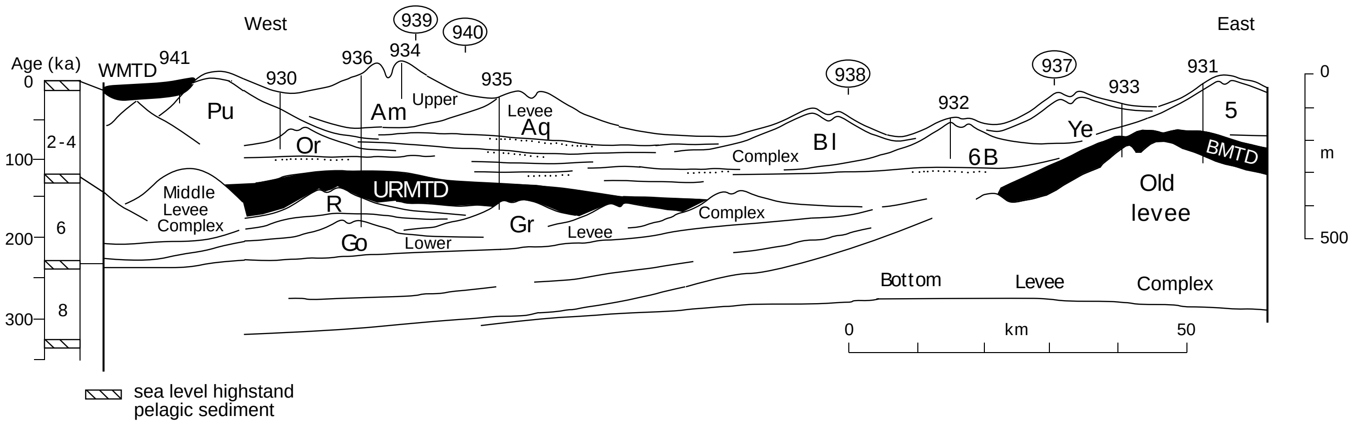

Figure 2. Schematic cross section of the Amazon Fan (after Flood, Piper, Klaus, et al., 1995). Levee complexes are made up of stacked channel-levee systems. The stacked channel-levee systems result from abrupt channel switching that generates new levee systems. Four levee complexes have been identified having large mass-transport deposits separating them.

Table 1. Summary of acoustic stratigraphic nomenclature of channel-levee systems on the Amazon Fan (after Flood, Piper, Klaus, et al., 1995).

	Western Fan	Central Fan	Eastern Fan
Upper Levee Complex (ULC) (isotope stage = 2–4)	Purple (= 2)	Amazon (=1) Brown (=1) Aqua (=1) Blue (=3) Yellow (=4) Orange*	Channel 5* Channel 6A* Channel 6B* Channel 6C*
Unit R mass-transport deposit (URMTD)			
Middle Levee Complex (MLC) (isotope stage = 6)	Red		
Inferred mass-transport deposit			
Lower Levee Complex (LLC) (isotope stage = 8)		Green Gold Lime Gray	
Bottom mass-transport deposit (BMTD)			
Bottom Levee Complex			Old levee

Note: * = age relationship unknown.

All samples had duplicate analyses performed to check reproducibility. Additional analyses were performed only if the silt size (3.9 μm) percentage varied by more than 2%. Additional analyses were required for about 20 samples. For this study, both mode size and cumulative percent data were used. All data were plotted according to previously assigned architectural units as cumulative percent. Mode size was plotted downhole and triangular plots of sand-silt-clay content constructed (Figs. 4, 5). For each architectural unit, the dominant mode size, the clay:silt:sand ratio, and the cumulative percent from every sample was arithmetically summed and averaged. The term “average mode,” “average clay:silt:sand ratio,” and “average cumulative percent” are used to describe this averaging. These average values were then used for comparisons among the various architectural units (Table 2).

Grain size for medium to coarse sand (<2 ø) samples were determined by a settling tube. Samples were introduced into suspension at the upper end of a 1-m settling tube and the grain-size determination used the Gibbs’ settling equation (Gibbs et al., 1971). The tube was calibrated using dry sieved samples of a well-rounded quartz (Jordan Sandstone).

OBSERVATIONS

Individual Sites

Site 930

Site 930 is located on the upper part of the Amazon Fan (Figs. 1, 2), between the levees of the buried Purple Channel and the Amazon Channel, and penetrated ~270 m through four channel-levee systems (Amazon, Purple, Blue/Yellow, and Orange), all part of the ULC. The dominant average mode size for the Amazon samples is 7.4 ø with clay:silt:sand ratio 14:80:6 and a fining-upward trend (Figs. 4, 5). A mass-transport unit, having an upper slope-outer shelf source (Flood, Piper, Klaus, et al., 1995), was encountered near the base of the hole within the Orange system. This mass-transport deposit contains two distinct blocks, each characterized by different grain sizes; the sandy mud unit has an average mode of ~4.8 ø (9:76:15), whereas the displaced block unit has an average mode of 8.2 ø (21:74:5). The coarser size occurs primarily at the top of the mass-transport unit.

Site 931

Located on the western levee of the buried Channel-levee 5 system on the eastern part of the Amazon Fan (Figs. 1, 2), Site 931 penetrated ~420 meters below seafloor (mbsf) into sediments from channel levees belonging to the ULC (Amazon/Blue/Yellow, and Channel 5), a HARP, a buried mass-transport deposit (named the bottom mass-transport deposit [BMTD], Piper et al., Chapter 6, this volume) and an older channel-levee system (termed “Old Levee” in this paper) belonging to the BLC. The levee system of the BLC shows a fining-upward sequence and an average mode size of 7.5 ø (16:80:4) (Fig. 4). The BMTD has a range in grain sizes (8.2 ø to 3.7 ø) that gives an average of the mode sizes for the unit of 7.1 ø and coarsens upward. The HARP unit contains sediments that separate into two grain-size populations; 6.6 ø and 3.5 ø. Channel 5 of the ULC has an average mode of 5.5 ø (12:85:3), and the overlying Amazon levee is finer (6.6 ø, 15:85:0).

Site 933

Located near Site 931, Site 933 is positioned on the eastern flank of the Yellow Channel-levee System (Figs. 1, 2). Sediments were recovered to a depth of ~250 mbsf. Acoustic units sampled include the Amazon/Blue, Yellow, Channel systems 5, 6A, and 6B of the ULC,

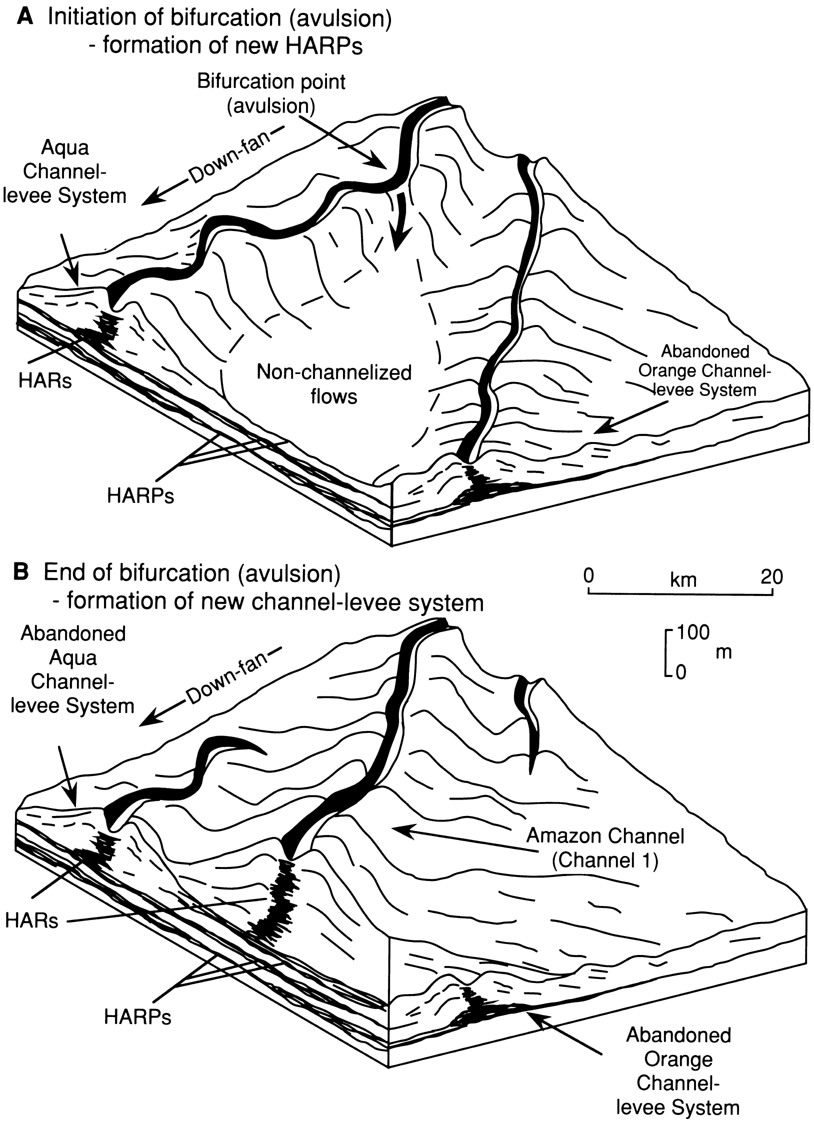

Figure 3. Schematic block diagram illustrating the development of a new channel-levee system (and associated HARPs) following an avulsion event (from Flood et al., 1991).

the BMTD, and the Old Levee of the BLC. Site 931 sampled the Old Levee on its eastern flank, whereas Site 933 sampled the levee ~ 8 km upfan and nearer its crest. The Old Levee of the BLC has a relatively consistent grain size with an average mode of 7.0 ø. The BMTD shows an overall fining-upward sequence with a distinct change in grain size between ~130 and 160 mbsf (Fig. 4). The ratio of clay:silt:sand remains similar for the older BLC levee and the BMTD between Sites 931 and 933 (Table 2). Channels 5, 6A, 6B have an average mode of 7.1 ø (14:84:2), and the overlying Yellow system is slightly coarser 6.8 ø (15:84:1). The Amazon/Blue system is the finest sediment at this site (7.8 ø, 17:83:0).

Site 935

Drilling through two of the stacked channel-levee complexes (ULC and LLC), Site 935 is located near the bifurcation of the Aqua system and the Amazon Channel (Figs. 1, 3). The Amazon and Aqua systems with associated HARP units were sampled within the ULC, whereas only the Green Channel-levee was sampled within the LLC. Between these two stacked complexes, the acoustic unit Unit R (URMTD of Piper et al., Chapter 6, this volume) was sampled. The Green levee has a consistent grain size with an average mode of 7.3 ø and an average clay:silt:sand ratio of 14:83:3. The mass-transport deposit, URMTD, is slightly coarser than the Green levee (7.1 ø; 15:79:6) and has three fining-upward sequences within it (Fig. 4). The HARP unit is composed of two distinct sediment types with differing grain sizes. The silty clay sediment has an average mode of 7.4 ø (clay:silt:sand ratio = 14:83:3), whereas the sandy sediment has an average mode of 1.1 ø (clay:silt:sand ratio = 0:1:99). The Aqua system shows a fining-upward trend and has an average mode of 7.0 ø with a clay:silt:sand ratio of 12:83:5. The overlying Amazon system dramatically shows a fining-upward sequence (average mode 7.6 ø) and has a greater proportion of clay (16:81:3) in comparison to the Aqua system (Fig. 4).

Site 936

Site 936 is located on the western flank of the Amazon channel upfan from the Brown bifurcation site (Figs. 1, 2). This site sampled three stacked levee complexes (ULC, MLC, LLC) and the mass-transport deposit, URMTD. Within the ULC, samples were obtained from the Amazon/Brown system and the underlying HARP unit. From the MLC the Red system was sampled, and the Gold system was sampled from the LLC. The Gold system (which avulsed to create the Green system [Manley and Flood, 1988]) has an average mode size of 7.1 ø with a clay:silt:sand ratio of 15:77:8. Although the Green system sampled at Site 935 had a consistent grain size, the Gold system has two fining-upward cycles. The overlying Red system of the MLC has an average mode size of 6.6 ø and a clay:silt:sand ratio of 10:82:8. URMTD has several fining-upward cycles with an average

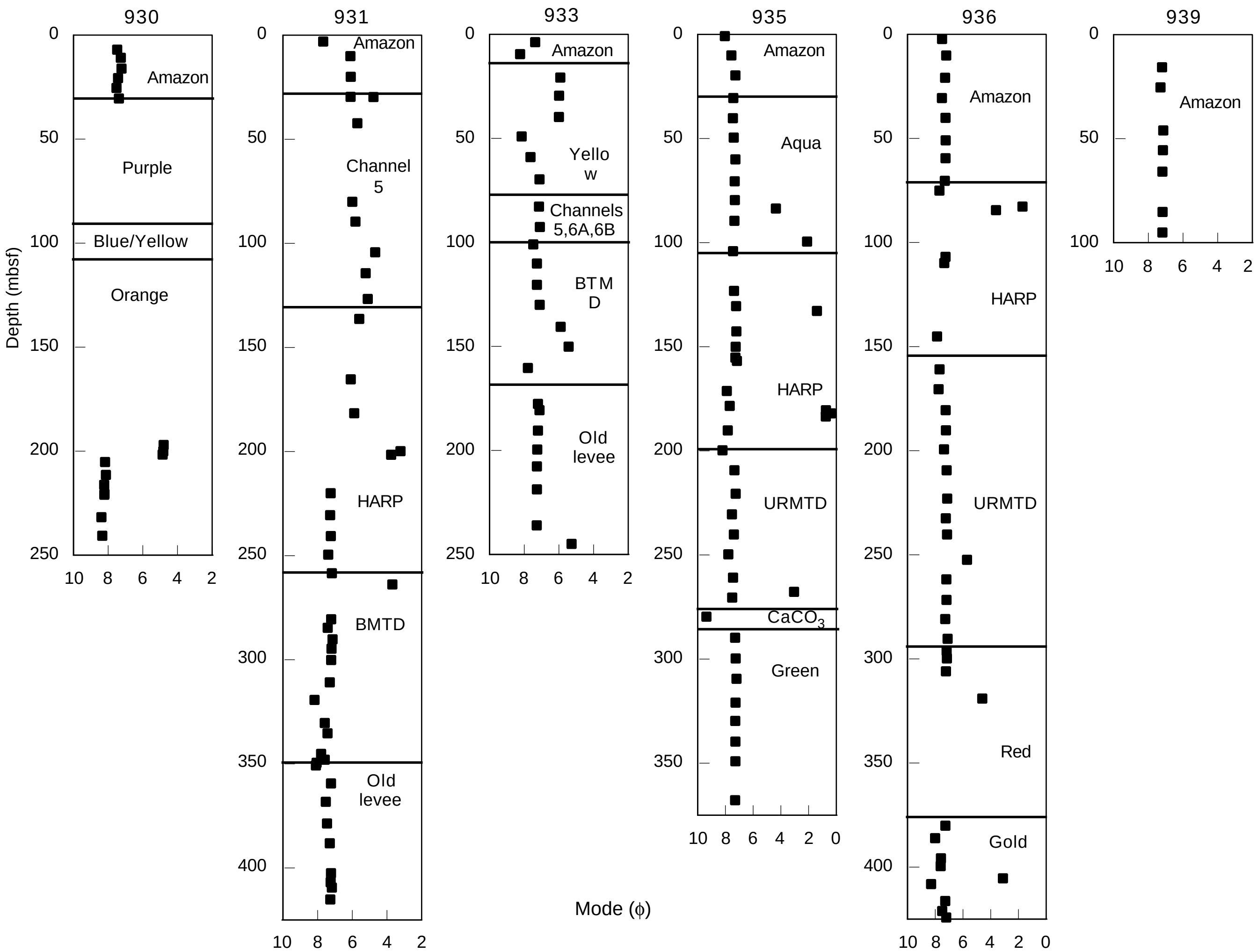

Figure 4. Downhole trends of grain-size mode determinations for discrete samples at individual sites. Seismic-facies units (or architectural units) are identified to allow for cross- and downfan correlation. Levees show an overall fining-upward trend, and at certain sites several fining-upward cycles are observed. Mass-transport deposits generally show a fining-upward trend, whereas HARs and HARPs are the coarsest material recovered from the fan.

mode of 7.2 ø (13:84:3). The HARP unit sampled is associated with the Amazon/Brown and Aqua systems of the ULC. Considering the unit as a whole, there are two dominant grain sizes that reflect the interfingered material recovered from this unit. Layers of finer grained sediment have an average mode size of 7.6 ø (clay:silt:sand ratio of 14:80:6), whereas the coarser grained sediment averages 2.7 ø (clay:silt:sand ratio of 0:14:86). The most recent channel-levee system, the Amazon, has two cycles of fining-upward having an average mode size of 7.3 ø (clay:silt:sand ratio of 14:84:2) (Figs. 4, 5).

Site 939

Located on the crest of the eastern levee of the Amazon Channel, this site sampled the Amazon system (ULC) in the region of the upper fan. Only penetrating ~100 mbsf, this site, in conjunction with sites 940, 944, and 946, allows for downfan trends to be examined. Grain size for the Amazon/Brown system has an average mode of 7.2 ø and a clay:silt:sand ratio of 12:83:5. Only one fining-upward sequence was observed (Figs. 4, 5).

Site 940

Site 940, located 60 km downfan from Site 939, penetrated the eastern levee of the Amazon system (ULC) and is located just upslope of the Aqua bifurcation site (Figs. 1, 2). This site records changes in deposition within the levee deposits in response to channel avulsions downslope. The Aqua system avulsed to create the Brown system, which in turn also experienced an avulsion event that led to the development of the Amazon system (Flood et al., 1991). Grain-size analysis of this site shows several stacked fining-upward sequences (Fig. 4). The two lowermost cycles are related to the Aqua system, which has an average mode of 6.6 ø and a clay:silt:sand ratio of 11:77:12. The overlying sediment corresponds to the transition period when both the Aqua and Brown systems were believed to be active (Pirmez and Flood, 1995). This interval also shows a fining-upward sequence, but has a slightly finer modal grain size (7.2 ø) than the Aqua system and a clay:silt:sand ratio that shows a decrease in the percentage of sand (13:82:5). The section that corresponds to the Brown system has an average mode size of 6.8 ø (clay:silt:sand ratio of 12:82:6), whereas the youngest sediment of the Amazon system has an average mode size of 7.2 ø and a clay:silt:sand ratio of 12:82:6.

Site 941

Site 941 is located on the western side of the Amazon deep-sea fan in a surficial debris flow originally described by Damuth and Embley (1981) (Figs. 1, 2). Site 941 recovered sediment from the western mass-transport deposit (WMTD) and the Purple Channel of the ULC. The Purple levee has an average mode size of 5.9 ø (14:86:0), which is coarser than the overlying WMTD (7.9 ø, 18:77:5). There is a

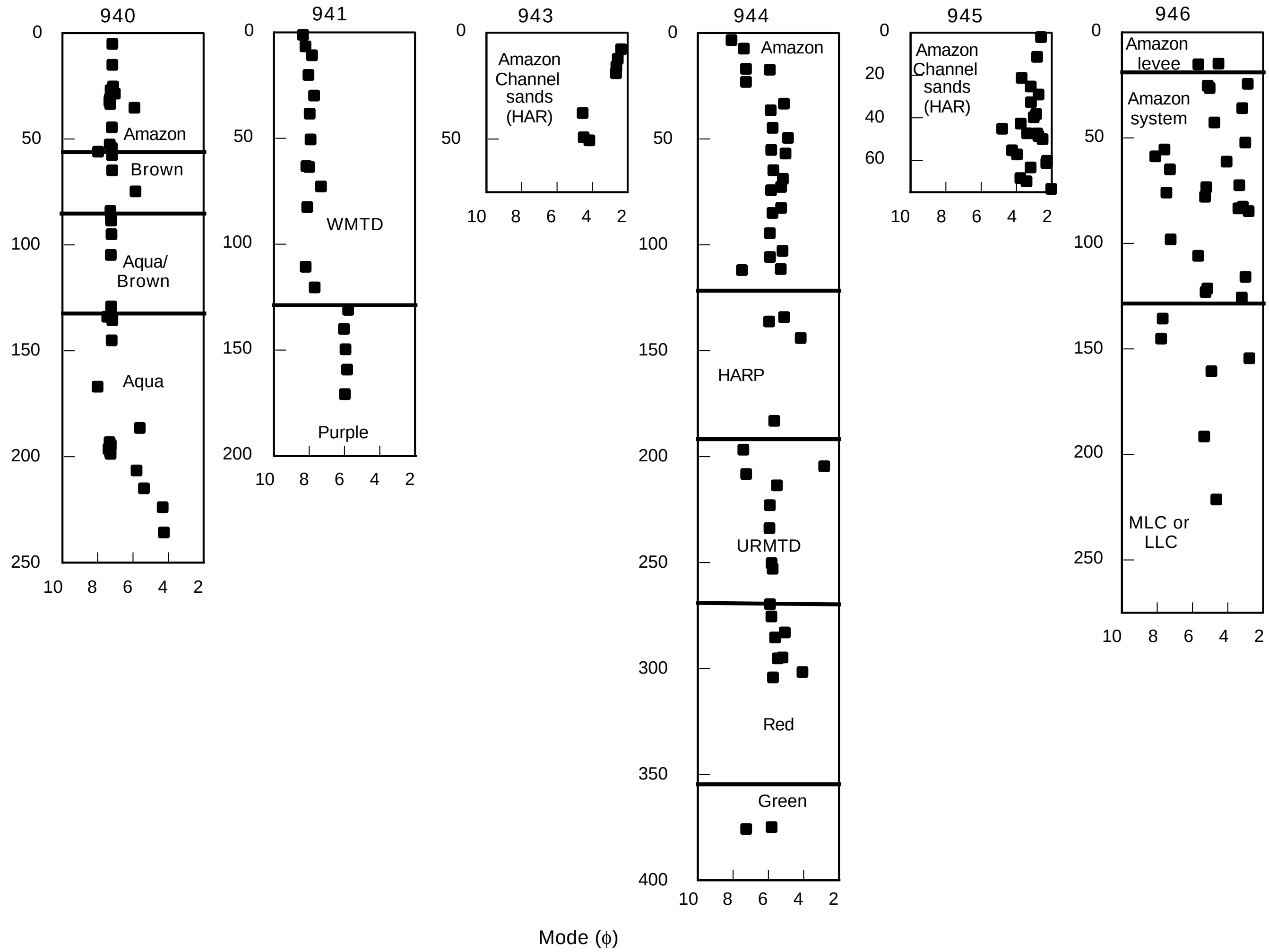

Figure 4 (continued).

slight coarsening-upward trend within the WMTD that is described in more detail in Piper et al. (Chapter 6, this volume).

Site 943

Located within the Amazon Channel on the middle fan, Site 943 recovered sediments that correlate to a HAR acoustic unit and some buried levee deposits. Grain-size analyses of samples that appear to be representative of the HAR unit contain two dominant grain sizes. The lowermost material recovered from the HAR unit was mostly silt, with an average mode of 4.4 ø, and a clay:silt:sand ratio of 0:72:28. The material recovered in the upper part of the HAR unit was much coarser (2.6 ø) and contained a high percentage of sand (0:9:91) (Figs. 3, 4; Table 2).

Site 944

Site 944 is located on the middle Amazon Fan on the eastern levee of the Amazon Channel, downfan from the Amazon/Brown avulsion (Pirmez and Flood, 1995) (Fig. 1). Site 944 sampled three stacked channel-levee complexes (ULC, MLC, LLC) and a mass-transport deposit, URMTD. The lowermost channel system sampled was the Green system from the LLC. Only two samples were analyzed, giving an average mode of 6.5 ø with a clay:silt:sand ratio of 13:80:7. Overlying the LLC, the Red Channel-levee System (MLC) is coarser than the Green system, having an average mode of 5.4 ø and a higher percentage of sand (10:73:17) with a slight fining-upward trend (Figs. 3, 4; Table 2). URMTD sediments lie directly above the Red system and are coarser than the URMTD sediments sampled at Site 936. At Site 944, the URMTD has an average mode of 5.8 ø and a clay:silt:sand ratio of 11:68:21. A distinct change in grain size occurs at ~220 mbsf within URMTD (Fig. 4). The lower portion of URMTD has a consistent grain size of ~5.8 ø and becomes finer by 1.5 ø above ~220 mbsf. The HARP unit was poorly recovered at Site 944 with less than 10% recovery in most cores. Four samples were analyzed having a similar grain size with an average mode size of 5.2 ø (8:74:18) from the recovered material. Grain size fluctuates within the Amazon/Brown system, but the unit displays an overall fining-up trend. The average mode size for the Amazon/Brown levee deposit is 6 ø with a clay:silt:sand ratio of 10:76:14.

Site 945

Located at the transition between the middle and lower portion of the Amazon Fan, Site 945 is positioned within the Amazon Channel thalweg. The interval between 0 and 10 mbsf is interpreted to be a channel-fill deposit (Flood, Piper, Klaus, et al., 1995). Two distinct grain-size populations are characteristic for this channel fill. One group of samples has an average mode of 3.4 ø (1:41:58), whereas the other group is coarser (2.4 ø; 0:14:86) (Fig. 4; Table 2).

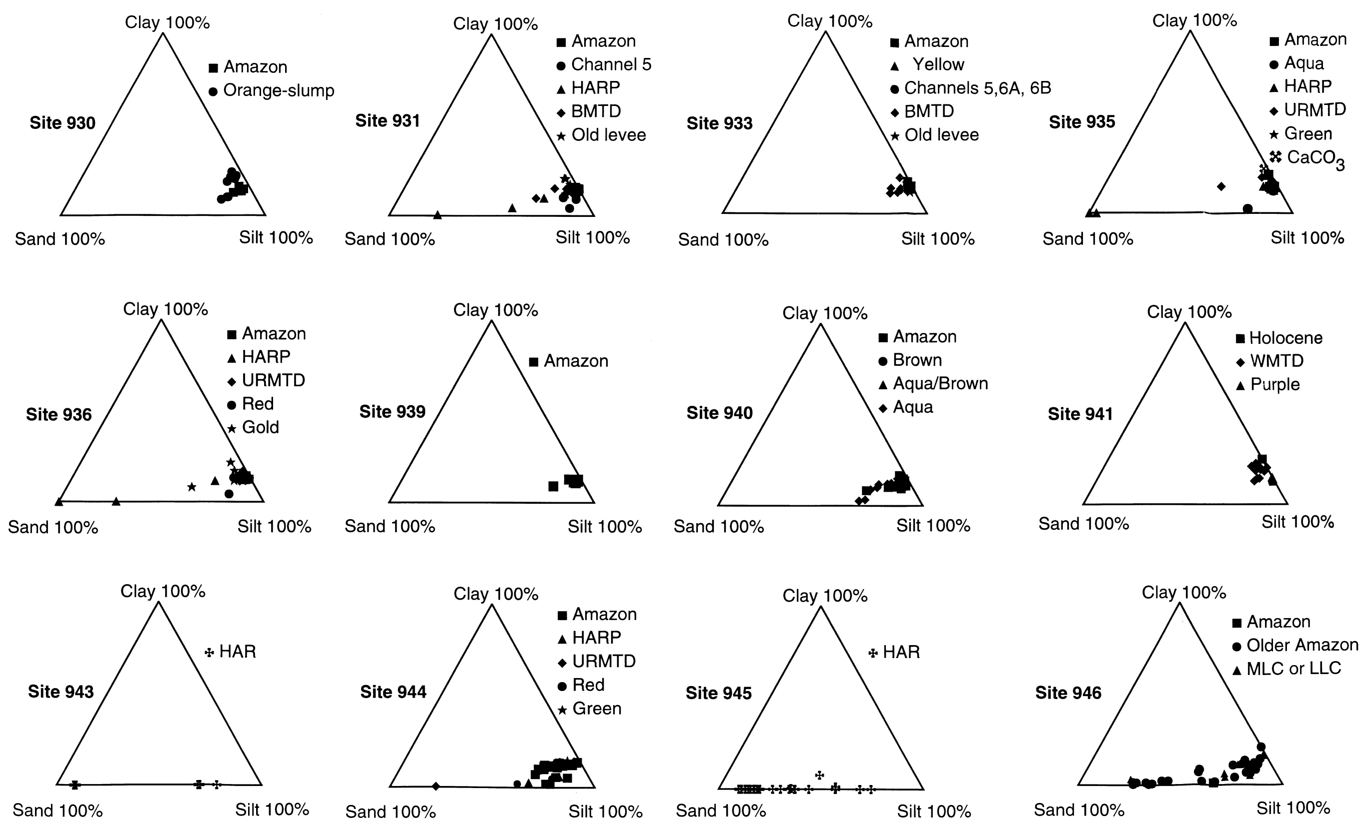

Figure 5. Triangular plot of sand-silt-clay content of discrete samples for individual sites. Different symbols represent the samples within the defined architectural units. Most sites show little variability in the relative proportions of sand-silt-clay.

Site 946

Site 946 is located on the Amazon levee flank, 1.2 km east of the channel thalweg sampled at Site 945 (Fig. 1). The upper 20 mbsf represent the most recent Amazon Channel-levee System, whereas, the remainder of the hole sampled older systems of the ULC as well as the MLC or LLC. Grain size for the Amazon Channel-levee System has an average mode of 5.1 ø with a clay:silt:sand ratio of 6:73:21 based on two samples. This is slightly finer than the units sampled below 20 mbsf. Between 20 and 125 mbsf, the grain size of the sediment ranges between 1.7 ø and 7.5 ø having an overall average mode of 4.7 ø with a clay:silt:sand ratio of 7:60:33. This interval overlies an older complex (either the MLC or LLC), which is coarser (5.5 ø), ranging between 2.8 ø and 7.8 ø, but has a similar clay:silt:sand ratio (8:66:26).

COMPARISON WITH ACOUSTIC UNITS

Grain size has long been used as an indicator of sedimentary environment as well as to assist in the understanding of sedimentary processes. Previous studies of submarine fans generally lacked the core information to ground truth the interpretation of seismic reflection profiles.

Four main architectural units comprise the bulk of the Amazon fan, channel levee systems (overbank deposits), large mass-transport deposits (MTDs), high-amplitude reflectors (HARs, Kastens and Shor, 1986), and high-amplitude reflection packets (HARPs, Flood et al., 1991) (Figs. 2, 3). Because the spatial distribution of these units is very well constrained on the Amazon Fan (Damuth et al., 1983a, 1983b; Damuth et al., 1988; Manley and Flood, 1988; Flood et al., 1991; Pirmez, 1994; Pirmez and Flood, 1995; Flood, Piper, Klaus, et al., 1995), average grain-size profiles for each acoustic unit, both downfan and crossfan, can be constructed from the drilled sites.

Grain-size analyses were determined for sediment samples correlated to the acoustic units identified at individual sites. Cumulative plots for samples allowed for characterization of grain size for those specific acoustic units (Fig. 6). Finally an overall cumulative average was determined for the key acoustic units at each site allowing for interhole comparisons between these architectural units (Table 2). By comparing downhole and downfan trends in grain size, the sediment and acoustic facies observed on the fan can be characterized and quantified (Figs. 4, 6–9).

Channel Levees

Channel levees are acoustically characterized by continuous to discontinuous parallel to subparallel reflections. Previous studies (Damuth, et al., 1983a, 1988; Manley and Flood, 1988; Flood et al., 1991) suggest that only one channel levee system is active at any given time and abandonment of an active channel by avulsion leads to the formation of a new channel levee nearby. Therefore, channel-levee systems grow both vertically and downfan (Fig. 3). Lithologically, levees sampled were generally composed of mud with thin beds and laminae of silt and sand.

At all sites, sediment within individual levees (from all levee complexes) contains distinct fining-upward sequences (Fig. 4). Several models have suggested that fining-upward or coarsening-upward trends are a response of sediment volume to modulation by sea-level or climatic mechanisms (Posamentier and Vail, 1988; Posamentier et al., 1991). Appi et al. (1988) utilized piston cores (10 to 20 m in length) to investigate sedimentological changes within the Amazon

Table 2. Grain-size data for Amazon Fan sediments.

Core, section, interval (cm)	Volume (cm^3)	Method (M or ST)	Depth (mbsf)	Mode (µm)	Mode (ø)	Clay (%)	Silt (%)	Sand (%)	Acoustic unit	Average mode (ø)	Average clay:silt:sand
155-930B-											
2H-1, 131–133	10	M	7.01	5.61	7.48	15.80	79.13	5.07	Amazon levee	7.38	14:80:6
2H–4, 71–73	10	M	10.91	6.47	7.27	13.24	81.65	5.11			
3H-1, 90–92	10	M	16.10	6.67	7.23	14.30	82.18	3.52			
3H-4, 98–100	10	M	20.68	5.80	7.43	13.49	81.19	5.32			
4H-1, 70–72	10	M	25.40	5.45	7.52	13.69	80.96	5.35			
4H-4, 127–129	10	M	30.47	6.00	7.38	12.53	78.15	9.32			
22X-1, 63–65	10	M	197.03	35.82	4.80	10.06	76.73	13.21	Mass transport	4.83	9:76:15
22X-3, 66–68	10	M	200.06	35.49	4.82	10.04	76.30	13.66		(sandy unit)	
22X-7, 68–70	10	M	205.22	3.44	8.18	21.68	74.25	4.07			
24X-1, 51–53	10	M	216.21	3.34	8.23	21.79	74.82	3.39		8.24	21:74:5
24X-4, 36–38	10	M	220.56	3.37	8.21	21.27	74.89	3.84		(displaced units)	
155-930C-											
13X-1, 53–56	10	M	201.63	34.50	4.86	8.78	74.08	17.14			
14X-1, 60–62	10	M	211.40	3.58	8.13	21.05	72.42	6.53			
15X-1, 54–56	10	M	220.94	3.36	8.22	20.02	74.97	5.01			
16X-2, 74–76	10	M	231.74	2.99	8.39	18.56	72.06	9.38			
17X-1, 96–98	10	M	240.66	3.09	8.34	23.89	71.61	4.50			
155-931B-											
2H-2, 76–78	10	M	3.06	4.89	7.68	15.69	83.20	1.11	Amazon/Blue/Yellow	6.62	15:85:0
2H-7, 27–29	10	M	10.07	14.48	6.11	15.04	84.96	0.00			
3H-7, 75–77	10	M	20.00	14.70	6.09	14.60	85.28	0.12			
5H-1, 32–34	10	M	29.62	14.54	6.10	15.42	84.58	0.00	Channel 5	5.45	12:85:3
5H-1, 41–43	10	M	29.71	36.38	4.78	4.18	86.02	9.80			
6H-3, 50–52	10	M	42.30	19.12	5.71	14.27	85.06	0.67			
10X-3, 23–25	10	M	80.03	15.66	6.00	14.43	85.38	0.19			
11X-4, 75–77	10	M	89.55	17.65	5.82	13.45	86.07	0.48			
13X-1, 78–80	10	M	104.28	38.95	4.68	9.97	80.14	9.89			
14X-1, 114–116	10	M	114.34	26.69	5.23	11.30	85.58	3.12			
15X-3, 90–92	10	M	126.70	29.03	5.11	9.08	86.70	4.22			
16X-3, 78–80	10	M	136.28	20.57	5.60	13.49	85.38	1.13			
19X-3, 80–82	10	M	165.30	14.69	6.09	15.51	84.38	0.11	HARP	3.49	2:41:57
21X-1, 89–91	10	M	181.59	16.81	5.89	14.85	84.91	0.24			
23X-1, 00–02	10	M	199.80	107.39	3.22	0.51	23.50	75.99		6.63	14:81:5
23X-2, 23–25	10	M	201.53	73.84	3.76	4.35	58.12	37.53			
25X-1, 90–92	10	M	220.00	6.56	7.25	13.98	85.65	0.37			
26X-2, 35–37	10	M	230.55	6.45	7.28	9.67	70.93	19.40			
27X-2, 69–71	10	M	240.59	6.62	7.24	12.86	82.74	4.40	BMTD	7.09	13:80:7
28X-2, 14–16	10	M	249.51	5.97	7.39	12.42	80.14	7.44			
29X-1, 74–76	10	M	258.44	6.90	7.18	11.13	79.58	9.29			
29X-5, 12–14	10	M	263.82	77.66	3.69	9.55	67.17	23.28			
31X-3, 64–66	10	M	280.54	6.71	7.22	14.77	79.26	5.97			
31X-6, 25–27	10	M	284.65	5.85	7.42	14.49	80.88	4.63			
32X-3, 58–60	10	M	290.18	7.11	7.14	13.78	83.32	2.90			
32X-6, 59–61	10	M	294.69	6.82	7.20	11.63	84.86	3.51			
33X-3, 91–93	10	M	300.11	6.70	7.22	14.86	82.07	3.07			
34X-4, 54–56	10	M	310.84	6.35	7.30	14.39	82.93	2.68			
35X-3, 78–80	10	M	319.28	3.44	8.18	15.00	73.45	11.55			
36X-4, 77–79	10	M	330.37	5.18	7.59	15.88	80.90	3.22			
37X-1, 52–54	10	M	335.32	5.78	7.43	15.53	80.58	3.89			
38X-1, 80–82	10	M	345.20	4.49	7.80	17.33	79.76	2.91	BLC—Old Levee	7.50	16:80:4
38X–3, 60–62	10	M	348.00	5.18	7.59	12.05	80.23	7.72			
38X-4, 57–59	10	M	349.47	3.76	8.06	20.64	75.29	4.07			
38X-5, 81–83	10	M	350.75	3.64	8.10	20.46	75.99	3.55			
39X-4, 79–81	10	M	359.39	6.65	7.23	15.26	82.31	2.43			
40X-4, 75–77	10	M	368.21	5.41	7.53	15.77	80.75	3.48			
41X-4, 73–75	10	M	378.63	5.66	7.46	14.73	80.80	4.47			
42X-4, 74–76	10	M	388.14	6.36	7.30	15.83	80.09	4.08			
44X-2, 14–16	10	M	402.51	6.68	7.23	15.74	81.62	2.64			
44X-5, 47–49	10	M	406.85	6.57	7.25	14.50	83.01	2.49			
44X-7, 47–49	10	M	409.42	6.88	7.18	14.93	80.95	4.12			
45X-3, 52–54	10	M	415.12	6.49	7.27	14.52	83.05	2.43			
155-933A-											
1H-3, 77–79	10	M	3.77	6.04	7.37	15.30	84.57	0.13	Amazon/Blue	7.81	17:83:0
2H-3, 61–63	10	M	9.52	3.30	8.24	17.56	81.67	0.77			
3H-5, 70–72	10	M	20.78	16.52	5.92	15.21	84.46	0.33	Yellow	6.80	15:84:1
4H-4, 30–32	10	M	29.50	15.73	5.99	13.41	86.30	0.29			
5H-4, 103–105	10	M	39.73	15.59	6.00	15.43	84.39	0.18			
6H-5, 58–60	10	M	49.08	3.52	8.15	16.70	82.73	0.57			
7H-8, 83–85	10	M	59.01	5.03	7.64	15.77	81.58	2.65			
8H-6, 66–68	10	M	69.71	7.21	7.12	13.55	84.72	1.73			
10H-1, 111–113	10	M	82.81	7.05	7.15	13.84	83.04	3.12	Channels 5, 6A, 6B	7.12	14:84:2
11X-1, 141–143	10	M	92.61	7.31	7.10	14.03	84.61	1.36			
12X-1, 117–119	10	M	100.97	5.60	7.48	19.55	76.61	3.84	BMTD	6.89	14:79:7
13X-1, 77–79	10	M	110.17	6.48	7.27	11.24	76.00	12.76			
14X-1, 140–142	10	M	120.40	6.48	7.27	11.55	79.58	8.87			
15X-1, 132–134	10	M	130.02	7.24	7.11	15.26	82.94	1.80			
16X-2, 79–81	10	M	140.59	16.74	5.90	13.59	79.97	6.44			
17X-2, 73–75	10	M	150.13	23.08	5.44	12.67	83.47	3.86			
18X-2, 128–130	10	M	160.38	4.53	7.79	13.89	75.02	11.09			
20X-1, 74–76	10	M	177.64	6.75	7.21	12.94	81.92	5.14	BLC—Old Levee	6.99	14:83:3
20X-3, 77–79	10	M	180.67	7.17	7.12	14.84	82.54	2.62			

Table 2 (continued).

Core, section, interval (cm)	Volume (cm^3)	Method (M or ST)	Depth (mbsf)	Mode (µm)	Mode (ø)	Clay (%)	Silt (%)	Sand (%)	Acoustic unit	Average mode (ø)	Average clay:silt:sand
21X-3, 98–100	10	M	190.48	6.77	7.21	14.71	83.17	2.12			
22X-3, 79–81	10	M	199.58	6.57	7.25	13.56	83.05	3.39			
23X-2, 121–123	10	M	207.70	6.47	7.27	16.65	81.38	1.97			
24X-3, 81–83	10	M	218.73	6.47	7.27	15.51	82.30	2.19			
26X-1, 124–126	10	M	236.04	6.43	7.28	13.70	83.55	2.75			
27X-1, 44–46	10	M	244.94	25.87	5.27	11.92	85.52	2.56			
155-934A-											
6H-3, 33–35	10	M	45.63	4.78	7.71	13.59	83.34	3.07	Channel slump	7.71	13:83:4
6H-6, 69–71	10	M	49.66	4.70	7.73	13.56	82.98	3.46			
7H-3, 60–62	10	M	55.40	4.96	7.66	12.35	82.36	5.29			
7H-6, 62–64	10	M	59.92	4.66	7.75	13.48	82.68	3.84			
155-935A-											
1H-1, 83–85	10	M	0.83	3.80	8.04	20.65	77.97	1.38	Amazon levee	7.63	16:81:3
2H-5, 59–61	10	M	10.09	5.26	7.57	14.16	81.82	4.02			
3H-5, 69–71	10	M	19.69	6.44	7.28	14.19	84.01	1.80			
4H-6, 56–58	10	M	30.56	5.78	7.43	14.56	82.16	3.28	Aqua levee	6.99	12:83:5
5H-6, 74–76	10	M	40.24	5.68	7.46	15.28	82.87	1.85			
6H-6, 56–58	10	M	49.56	5.92	7.40	14.29	83.72	1.99			
7H-7, 44–46	10	M	60.02	6.43	7.28	12.20	84.67	3.13			
9H-1, 54–56	10	M	70.54	6.23	7.33	13.89	84.16	1.95			
9H-7, 56–58	10	M	79.56	6.26	7.32	13.37	84.55	2.08			
10H-4, 40–42	10	M	83.61	48.78	4.36	2.28	77.01	20.71			
11H-1, 52–54	10	M	89.52	6.11	7.35	13.34	83.60	3.06			
12H-1, 99–101	10	M	99.49	231.65	2.11	0.00	3.40	96.60	HARP	1.08	0:1:99
12H-4, 111–113	10	M	104.11	5.70	7.45	13.07	82.77	4.16			
15X-1, 87–89	10	M	123.17	6.00	7.38	15.00	83.69	1.31		7.44	14:83:3
15X-6, 70–72	10	M	130.50	6.68	7.23	14.25	84.16	1.59			
16X-1, 80–82	10	ST	132.80	380.00	1.40	0.00	0.00	100.00			
17X-1, 92–94	10	M	142.62	6.76	7.21	13.34	82.82	3.84			
17X-6, 82–84	10	M	150.02	6.52	7.26	13.76	84.68	1.56			
18X-3, 82–84	10	M	155.22	6.42	7.28	14.34	83.43	2.23			
18X-4, 90–92	10	M	156.80	6.93	7.17	12.30	84.68	3.02			
20X-1, 84–86	10	M	171.24	4.18	7.90	18.44	80.11	1.45			
20X-6, 51–53	10	M	178.41	4.84	7.69	14.42	79.94	5.64			
21X-1, 50–52	10	ST	180.50	595.00	0.75	0.00	0.00	100.00			
21X-2, 50–52	10	ST	182.00	770.00	0.38	0.00	0.00	100.00			
21X-3, 50–52	10	ST	183.50	590.00	0.76	0.00	0.00	100.00			
22X-1, 58–60	10	M	190.18	4.41	7.83	14.57	78.47	6.96			
23X-1, 44–46	10	M	199.74	3.37	8.21	19.45	75.28	5.27	URMTD	7.06	15:79:6
24X-1, 32–34	10	M	209.32	6.15	7.35	13.28	83.11	3.61			
25X-2, 49–51	10	M	220.59	6.54	7.26	16.93	82.11	0.96			
26X-2, 79–81	10	M	230.49	5.42	7.53	16.32	81.88	1.80			
27X-2, 86–88	10	M	240.16	5.97	7.39	14.33	82.56	3.11			
28X-2, 79–81	10	M	249.69	4.51	7.79	15.61	81.61	2.78			
29X-3, 79–81	10	M	260.89	5.73	7.45	15.09	83.34	1.57			
30X-1, 100–102	10	M	267.70	121.14	3.05	14.75	57.91	27.34			
30X-3, 77–79	10	M	270.47	5.49	7.51	13.36	82.26	4.38			
31X-3, 33–35	10	M	279.63	1.51	9.37	24.17	73.85	1.98	$CaCO_3$ layer		
32X-3, 75–77	10	M	289.75	6.34	7.30	14.87	83.71	1.42	LLC—Green levee	7.27	14:83:3
33X–3, 100–102	10	M	299.70	6.51	7.26	14.28	83.21	2.51			
34X–3, 116–118	10	M	309.46	6.79	7.20	13.86	83.63	2.51			
35X–4, 142–144	10	M	320.92	6.50	7.27	14.32	82.06	3.62			
36X–4, 50–52	10	M	329.70	6.37	7.29	13.04	83.01	3.95			
37X–4, 84–86	10	M	339.64	6.43	7.28	13.74	84.32	1.94			
38X–4, 68–70	10	M	349.08	6.43	7.28	13.25	83.79	2.96			
40X–4, 28–30	10	M	367.78	6.34	7.30	14.67	83.39	1.94			
155-936A-											
1H-2, 76–78	10	M	2.26	5.50	7.51	14.38	84.03	1.59	Amazon levee	7.33	14:84:2
2H-3, 68–70	10	M	10.18	6.76	7.21	12.47	86.52	1.01			
3H-4, 43–45	10	M	20.88	6.40	7.29	13.64	84.14	2.22			
4H-4, 62–64	10	M	30.62	5.46	7.52	14.37	83.18	2.45			
5H-4, 63–65	10	M	40.13	6.51	7.26	13.86	81.99	4.15			
6H-5, 43–45	10	M	50.93	6.56	7.25	12.18	84.99	2.83			
7H-5, 6–8	10	M	59.52	6.51	7.26	13.11	84.94	1.95			
8H-5, 87–89	10	M	70.37	6.32	7.31	14.14	84.25	1.61			
9H-2, 57–59	10	M	75.07	4.80	7.70	11.59	70.42	17.99	HARP	7.55	14:80:6
10H-1, 24–25	10	ST	82.74	305.00	1.71	0.00	0.00	100.00			
10H-2, 46–47	10	M	84.46	81.38	3.62	0.27	27.92	71.81			
13X-1, 59–61	10	M	106.89	6.52	7.26	13.90	84.14	1.96		2.67	0:14:86
13X-3, 57–59	10	M	109.87	6.11	7.35	13.88	84.64	1.48			
17X-1, 33–35	10	M	145.13	4.26	7.87	16.25	81.49	2.26			
18X-1, 42–44	10	M	160.92	4.83	7.69	13.82	80.33	5.85	URMTD	7.18	13:84:3
19X-5, 37–39	10	M	170.47	4.60	7.76	16.99	81.31	1.70			
20X-5, 73–75	10	M	180.53	6.55	7.25	12.77	84.38	2.85			
21X-5, 81–83	10	M	190.21	6.66	7.23	12.59	85.00	2.41			
22X-5, 24–26	10	M	199.34	6.04	7.37	12.16	82.94	4.90			
23X-5, 61–63	10	M	209.41	6.89	7.18	11.61	85.34	3.05			
25X-1, 90–92	10	M	223.00	7.10	7.14	12.81	84.73	2.46			
26X-1, 77–79	10	M	232.47	6.62	7.24	12.94	83.94	3.12			
26X-6, 104–106	10	M	240.24	7.02	7.15	13.31	86.53	0.16			
28X-1, 130–132	10	M	252.40	19.05	5.71	11.50	82.52	5.98			
29X-1, 109–111	10	M	261.79	6.81	7.20	14.21	84.57	1.22			
30X-1, 126–128	10	M	271.66	6.86	7.19	13.34	83.19	3.47			

Table 2 (continued).

Core, section, interval (cm)	Volume (cm^3)	Method (M or ST)	Depth (mbsf)	Mode (µm)	Mode (ø)	Clay (%)	Silt (%)	Sand (%)	Acoustic unit	Average mode (ø)	Average clay:silt:sand
31X-1, 96–98	10	M	280.86	6.43	7.28	13.49	80.86	5.65			
32X-1, 94–96	10	M	290.34	7.22	7.11	15.66	81.66	2.68			
32X-5, 69–71	10	M	296.09	6.89	7.18	12.18	84.03	3.79	MLC—Red levee	6.55	10:82:8
33X–1, 78–80	10	M	299.78	6.97	7.16	12.65	82.96	4.39			
33X–5, 96–98	10	M	305.96	6.65	7.23	13.27	78.68	8.05			
35X–1, 85–87	10	M	319.05	40.91	4.61	4.29	80.86	14.85			
41X–3, 111–113	10	M	380.11	6.48	7.27	13.21	81.93	4.86	LLC—Gold levee	7.10	15:77:8
42X-1, 40–42	10	M	386.10	3.88	8.01	17.27	77.06	5.67			
43X-1, 47–49	10	M	395.77	5.18	7.59	13.61	80.47	5.92			
43X-4, 39–41	10	M	399.53	5.13	7.61	15.76	80.42	3.82		7.59	15:79:5
44X-1, 39–41	10	M	405.39	115.31	3.12	8.23	60.80	30.97		w/o sand layer	
44X-3, 15–17	10	M	408.15	3.18	8.30	21.77	72.92	5.31			
45X-2, 95–97	10	M	416.29	6.45	7.28	11.72	79.69	8.59			
45X-6, 106–108	10	M	421.09	5.53	7.50	15.11	80.80	4.09			
46X-1, 20–22	10	M	424.20	6.76	7.21	13.24	81.28	5.48			
155-939B-											
3H-3, 34–36	10	M	15.68	6.77	7.21	10.80	85.60	3.60	Amazon levee	7.20	12:83:5
4H-2, 85–87	10	M	25.35	6.34	7.30	12.80	81.40	5.80			
6H-4, 83–85	10	M	46.04	7.09	7.14	9.10	75.60	15.30			
7H-4, 88–90	10	M	55.55	6.98	7.16	11.30	84.40	4.30			
8H-5, 90–92	10	M	65.85	6.85	7.19	11.80	84.60	3.60			
10X-4, 73–75	10	M	85.23	6.88	7.18	11.60	86.30	2.10			
11X-4, 90–92	10	M	95.10	6.87	7.19	12.80	85.80	1.40			
155-940A-											
2H-2, 79–81	10	M	5.09	6.95	7.17	10.30	80.60	9.10	Amazon levee	7.18	12:82:6
3H-2, 117–119	10	M	14.97	6.96	7.17	10.90	86.20	2.90			
4H-3, 38–40	10	M	25.18	7.14	7.13	8.30	68.30	23.40			
4H-4, 67–69	10	M	26.97	6.49	7.27	14.42	83.26	2.32			
4H-5, 76–78	10	M	28.56	7.63	7.03	9.42	84.69	5.89			
4H-7, 43–45	10	M	31.23	6.26	7.32	12.72	83.29	3.99			
5H-1, 96–98	10	M	32.26	6.17	7.34	13.85	84.22	1.93			
5H-2, 87–89	10	M	33.47	6.41	7.29	13.46	84.19	2.35			
5H-4, 9–11	10	M	35.23	16.46	5.92	10.80	84.90	4.30			
6H-3, 69–71	10	M	44.49	6.81	7.20	10.10	78.00	11.90			
7H-3, 17–19	10	M	52.58	6.27	7.32	14.91	83.02	2.07			
7H-4, 39–41	10	M	54.30	6.78	7.20	13.72	82.28	4.00			
7H-5, 63–65	10	M	55.97	3.95	7.98	16.70	80.20	3.10			
7H-6, 76–78	10	M	57.60	6.86	7.19	11.88	83.25	4.87			
8H-4, 49–51	10	M	64.79	6.90	7.18	10.40	79.40	10.20	Brown levee	6.77	12:82:6
9X-4, 93–95	10	M	74.73	17.24	5.86	11.60	81.70	6.70			
10X-5, 96–98	10	M	83.96	6.43	7.28	13.93	83.75	2.32			
11X-2, 85–87	10	M	87.05	6.54	7.26	12.50	81.36	6.14	Aqua/Brown	7.24	13:82:5
11X-3, 83–85	10	M	88.50	6.60	7.24	13.42	83.77	2.81	Transition		
12X-1, 64–66	10	M	94.94	6.70	7.22	11.30	80.40	8.30			
13X-1, 84–86	10	M	104.74	6.54	7.26	13.70	82.20	4.10			
15X-4, 124–126	10	M	129.04	6.63	7.24	13.43	82.75	3.82			
16X-1, 92–94	10	M	133.92	5.66	7.46	12.38	82.26	5.36	Aqua levee	6.56	11:77:12
16X-2, 104–106	10	M	135.54	6.93	7.17	8.90	70.00	21.10			
17X-2, 96–98	10	M	145.06	6.74	7.21	10.10	72.60	17.30			
19X-4, 54–56	10	M	166.94	3.88	8.01	14.90	80.20	4.90			
21X-4, 82–84	10	M	186.42	20.34	5.62	12.00	76.70	11.30			
22X-2, 84–86	10	M	193.14	6.21	7.33	13.01	81.93	5.06			
22X-3, 67–69	10	M	194.47	6.52	7.26	12.02	82.42	5.56			
22X-4, 106–108	10	M	196.36	5.97	7.39	12.80	82.40	4.80			
22X-5, 104–106	10	M	197.84	6.34	7.30	13.01	82.67	4.32			
22X-6, 34–36	10	M	198.64	6.48	7.27	12.82	84.79	2.39			
23X-5, 46–48	10	M	206.49	17.93	5.80	12.40	78.40	9.20			
24X-4, 43–45	10	M	214.93	24.04	5.38	11.70	72.60	15.70			
25X-3, 131–133	10	M	223.84	50.18	4.32	3.40	70.10	26.50			
26X-5, 47–49	10	M	235.77	52.42	4.25	2.70	67.50	29.80			
155-941A-											
1H-1, 114–116	10	M	1.14	3.07	8.35	24.79	75.17	0.04	Holocene		
2H-2, 104–106	10	M	6.60	3.38	8.21	20.27	79.69	0.04	WMTD	7.93	18:77:5
2H-5, 74–76	10	M	10.80	4.35	7.84	18.22	79.50	2.28			
3H-4, 78–80	10	M	20.08	3.81	8.04	20.27	76.40	3.33			
4H-4, 104–105	10	M	29.82	4.75	7.72	14.38	79.03	6.59			
5H-4, 36–38	10	M	38.36	3.98	7.97	19.44	76.76	3.80			
6H-6, 95–97	10	M	50.53	4.13	7.92	18.59	74.98	6.43			
8X-1, 85–87	10	M	63.15	3.49	8.16	20.90	71.78	7.32			
8X-1, 126–128	10	M	63.56	3.90	8.00	19.14	77.32	3.54			
9X-1, 94–96	10	M	72.74	6.22	7.33	12.88	77.25	9.87			
10X-1, 116–118	10	M	82.46	3.61	8.11	20.17	75.09	4.74			
13X-1, 37–39	10	M	110.67	3.40	8.20	22.53	73.16	4.31			
14X-1, 41–43	10	M	120.41	4.83	7.69	14.30	77.93	7.77			
15X-1, 129–131	10	M	130.99	18.07	5.79	12.68	86.67	0.65	Purple	5.92	14:86:0
16X-1, 67–69	10	M	139.97	15.32	6.03	14.98	84.87	0.15			
17X-1, 72–74	10	M	149.62	16.30	5.94	14.22	85.52	0.26			
18X-1, 61–63	10	M	159.21	17.37	5.85	13.56	85.94	0.50			
19X-2, 110–112	10	M	170.80	15.80	5.98	13.96	85.89	0.15			
155-943A-											
2H-3, 49–51	10	M	7.79	193.30	2.37	0.00	8.36	91.64	Amazon HAR	2.56	0:9:91
2H-6, 49–51	10	M	12.29	169.22	2.56	0.00	9.62	90.38			
3H-2, 70–72	10	M	16.00	160.16	2.64	0.00	9.40	90.60			

Table 2 (continued).

Core, section, interval (cm)	Volume (cm^3)	Method (M or ST)	Depth (mbsf)	Mode (µm)	Mode (ø)	Clay (%)	Silt (%)	Sand (%)	Acoustic unit	Average mode (ø)	Average clay:silt:sand
3H-4, 74–76	10	M	19.04	157.74	2.66	0.00	9.05	90.95			
5H-4, 45–47	10	M	37.75	42.76	4.55	0.00	78.18	21.82		4.41	0:72:28
7X-1, 90–92	10	M	49.17	44.40	4.49	0.00	69.07	30.93			
7X-2, 29–31	10	M	50.59	55.39	4.17	0.00	69.92	30.08			
155-944A-											
1H-3, 32–34	10	M	3.32	3.68	8.09	12.45	69.48	18.10	Amazon/Brown levee	5.97	10:76:14
2H-3, 43–45	10	M	7.33	5.95	7.39	11.26	72.74	16.00			
3H-3, 49–51	10	M	16.89	6.46	7.27	13.42	84.43	2.10			
3H-3, 90–96	50	M	17.30	16.57	5.92	11.72	78.63	9.65			
3H-7, 67–69	10	M	23.07	6.50	7.27	13.58	75.99	10.43			
5H-1, 92–98	50	M	33.32	28.71	5.12	10.91	76.28	12.81			
5H-3, 106–108	10	M	36.46	17.09	5.87	13.87	84.63	1.50			
6H-3, 24–26	10	M	44.74	18.44	5.76	9.88	70.36	19.76			
6H-7, 7–13	50	M	49.48	33.69	4.89	5.33	84.02	10.65			
7H-3, 78–80	10	M	55.18	17.40	5.84	12.86	82.07	5.07			
7H-4, 97–103	50	M	56.87	30.64	5.03	1.86	77.25	20.90			
8H-3, 86–88	10	M	64.76	18.92	5.72	13.13	75.60	11.27			
8H-6, 65–71	50	M	68.82	27.60	5.18	5.59	78.25	16.16			
9H-2, 75–81	50	M	72.65	25.70	5.28	11.53	72.07	16.40			
9H-3, 81–83	10	M	74.21	17.35	5.85	10.22	67.55	22.23			
10H-2, 117–124	50	M	82.57	25.81	5.28	1.98	75.18	22.84			
10H-4, 53–55	10	M	84.93	18.36	5.77	11.91	71.69	16.40			
11H-4, 60–62	10	M	94.50	16.52	5.92	12.04	74.07	13.89			
12X-4, 124–131	50	M	102.84	27.14	5.20	7.19	67.53	25.28			
13X-1, 82–84	10	M	105.72	16.64	5.91	11.13	75.98	12.89			
13X-5, 56–64	50	M	111.42	25.44	5.30	12.13	83.05	4.82			
13X-5, 106–108	10	M	111.92	5.54	7.50	11.58	69.53	18.89			
16X-1, 30–36	50	M	134.10	28.96	5.11	5.98	79.58	14.44	HARP	5.23	8:74:18
16X-2, 89–91	10	M	136.19	16.11	5.96	14.38	82.81	2.81			
17X-1, 58–60	10	M	143.98	55.49	4.17	2.67	66.52	30.81			
21X-1, 108–110	10	M	183.08	19.66	5.67	9.63	67.15	23.22			
22X-4, 60–62	10	M	196.70	5.84	7.42	13.50	76.31	10.19	URMTD	5.81	11:68:21
23X-3, 34–40	50	M	204.54	139.72	2.84	0.34	22.33	77.33			
23X-5, 99–101	10	M	208.19	6.53	7.26	14.01	76.05	9.94			
24X-2, 116–118	10	M	213.56	21.76	5.52	12.99	75.91	11.10			
25X-2, 91–93	10	M	222.91	16.54	5.92	10.66	70.07	19.27			
26X-3, 64–66	10	M	233.74	16.27	5.94	13.31	78.92	7.77			
28X-1, 87–93	50	M	250.27	17.76	5.82	10.69	71.83	17.48			
28X-3, 51–53	10	M	252.91	18.39	5.76	12.11	72.50	15.39			
30X-1, 94–96	10	M	269.64	16.61	5.91	13.20	74.33	12.47	MLC—Red	5.36	10:73:17
30X–6, 22–24	10	M	275.45	17.59	5.83	11.29	72.49	16.22			
31X–4, 100–106	40	M	283.00	29.84	5.07	4.78	76.76	18.46			
31X-6, 37–39	10	M	285.37	20.36	5.62	11.06	71.35	17.59			
32X-5, 144–150	50	M	294.81	27.13	5.20	10.46	68.54	21.00			
32X-6, 37–39	10	M	295.24	22.56	5.47	13.20	83.20	3.60			
33X-3, 109–115	40	M	301.69	59.74	4.07	2.03	61.30	36.67			
33X-5, 67–69	10	M	304.22	18.74	5.74	12.58	81.03	6.39			
41X-1, 40–46	50	M	374.90	17.72	5.82	12.07	79.69	8.24	LLC—Green	6.54	13:80:7
41X–1, 130–132	10	M	375.80	6.53	7.26	14.75	79.33	5.92			
155-945A-											
1H-2, 57–59	10	M	2.07	163.70	2.61	0.00	12.98	87.02	Amazon HAR	3.40	1:41:59
2H-2, 85–87	10	M	11.35	140.31	2.83	0.00	13.05	86.95			
3H-2, 122–124	10	M	21.22	76.57	3.71	0.00	37.40	62.60			
3H-5, 78–80	10	M	25.28	109.85	3.19	0.48	35.18	64.34			
4H-1, 105–107	10	M	29.05	148.40	2.75	0.00	26.45	73.55		2.43	0:14:86
4H-4, 22–24	10	M	32.72	110.05	3.18	7.87	45.42	46.71			
5H-1, 72–74	10	M	38.22	136.24	2.88	0.00	17.40	82.60			
5H-2, 72–74	10	M	39.72	123.06	3.02	0.00	26.50	73.50			
5H-4, 69–71	10	M	42.69	73.97	3.76	1.44	56.49	42.07			
5H-6, 14–16	10	M	45.14	35.61	4.81	0.00	74.44	25.56			
5H-7, 78–80	10	M	47.28	94.49	3.40	0.00	34.54	65.46			
6H-1, 33–35	10	M	47.33	140.63	2.83	0.00	20.20	79.80			
6H-2, 83–85	10	M	48.54	147.45	2.76	0.00	11.23	88.77			
6H-3, 83–85	10	M	50.04	174.91	2.52	0.00	15.49	84.51			
6H-4, 76–78	10	M	51.47	253.56	1.98	0.00	10.84	89.16			
6H-7, 43–45	10	M	55.27	52.66	4.25	0.00	68.97	31.03			
7H-1, 72–74	10	M	57.22	63.99	3.97	0.00	57.08	42.92			
7H-3, 72–74	10	M	60.22	207.88	2.27	0.00	19.35	80.65			
7H-4, 27–29	10	M	61.27	201.69	2.31	0.00	18.81	81.19			
7H-5, 84–86	10	M	63.34	108.84	3.20	0.00	37.08	62.92			
8H-1, 82–84	10	M	66.82	270.38	1.89	0.00	9.89	90.11			
8H-2, 84–86	10	M	68.34	72.68	3.78	0.00	44.13	55.87			
8H-3, 85–87	10	M	69.85	92.93	3.43	0.00	30.33	69.67			
8H-5, 141–143	10	M	73.41	245.47	2.03	0.00	17.26	82.74			
8H-6, 113–115	10	M	74.63	255.75	1.97	0.00	14.51	85.49			
155-946A-											
2H-6, 24–30	50	M	14.79	43.40	4.53	1.15	65.62	33.23	Amazon levee	5.10	6:73:21
2H-6, 58–60	10	M	15.13	19.62	5.67	10.38	80.80	8.82			
3H-6, 38–40	10	M	24.38	136.98	2.87	6.96	55.27	37.77	Older Amazon systems	4.71	7:60:33
3H-6, 128–135	50	M	25.28	28.44	5.14	10.86	77.56	11.58			
4H-1, 39–47	50	M	26.39	30.55	5.03	4.12	74.42	21.46			
5H-1, 41–43	10	M	35.91	110.70	3.18	2.32	42.58	55.10			
5H-5, 120-127	50	M	42.70	36.80	4.76	6.31	80.99	12.70			
6H–5, 120–127	50	M	52.20	123.75	3.01	8.53	55.09	36.38			
7H-1, 100–102	10	M	55.50	5.18	7.59	13.29	74.92	11.79			

Table 2 (continued).

Core, section, interval (cm)	Volume (cm^3)	Method (M or ST)	Depth (mbsf)	Mode (µm)	Mode (ø)	Clay (%)	Silt (%)	Sand (%)	Acoustic unit	Average mode (ø)	Average clay:silt:sand
7H-3, 125–131	50	M	58.75	3.61	8.11	20.56	79.36	0.08			
7H-5, 75–81	50	M	61.25	59.42	4.07	1.82	59.41	38.77			
8H-1, 90–92	10	M	64.90	6.43	7.28	12.05	80.22	7.73			
8H-6, 94–100	50	M	72.44	98.22	3.35	2.34	39.48	58.18			
8H-7, 34–41	50	M	73.35	26.74	5.22	6.72	78.83	14.45			
9H-2, 92–94	10	M	75.92	5.61	7.48	14.27	81.93	3.80			
9H-3, 139–145	50	M	77.89	25.58	5.29	11.36	74.84	13.80			
9H-7, 7–15	50	M	82.57	113.02	3.15	0.79	35.51	63.70			
10H-1, 39–47	50	M	83.39	94.52	3.40	0.42	34.04	65.54			
10H-2, 20–27	50	M	84.70	141.76	2.82	0.47	26.53	73.00			
10H-2, 78–80	10	M	85.28	319.43	1.65	1.38	27.63	70.99			
11H-4, 108–110	10	M	98.08	6.62	7.24	11.33	82.35	6.32			
12H-3, 88–90	10	M	105.88	19.45	5.68	8.39	82.64	8.97			
13H-3, 135–137	10	M	115.85	124.58	3.00	1.57	25.83	72.60			
14H-1, 34–40	50	M	121.34	27.91	5.16	1.91	65.82	32.27			
14H-2, 100–106	50	M	123.03	26.16	5.26	10.73	70.39	18.88			
14H-4, 60–62	10	M	125.63	108.02	3.21	1.36	32.25	66.39			
15H-4, 125–127	10	M	135.62	4.83	7.69	16.05	82.51	1.44	MLC or LLC	5.53	8:66:26
16X-4, 61–63	10	M	145.11	4.56	7.78	10.91	72.76	16.33			
17X-4, 32–34	10	M	154.42	145.29	2.78	3.15	24.05	72.80			
18X-1, 137–143	50	M	160.57	32.82	4.93	5.07	81.51	13.42			
21X-3, 29–36	50	M	191.49	24.77	5.34	6.13	68.44	25.43			
24X-3, 125–132	50	M	221.35	39.88	4.65	4.16	69.62	26.22			

Notes: M = grain-size analysis done on the Malvern MasterSizer E. ST = grain-size analysis done with a settling tube. Average mode and clay:silt:sand are the arithmetically averaged discrete samples for the indicated acoustic unit.

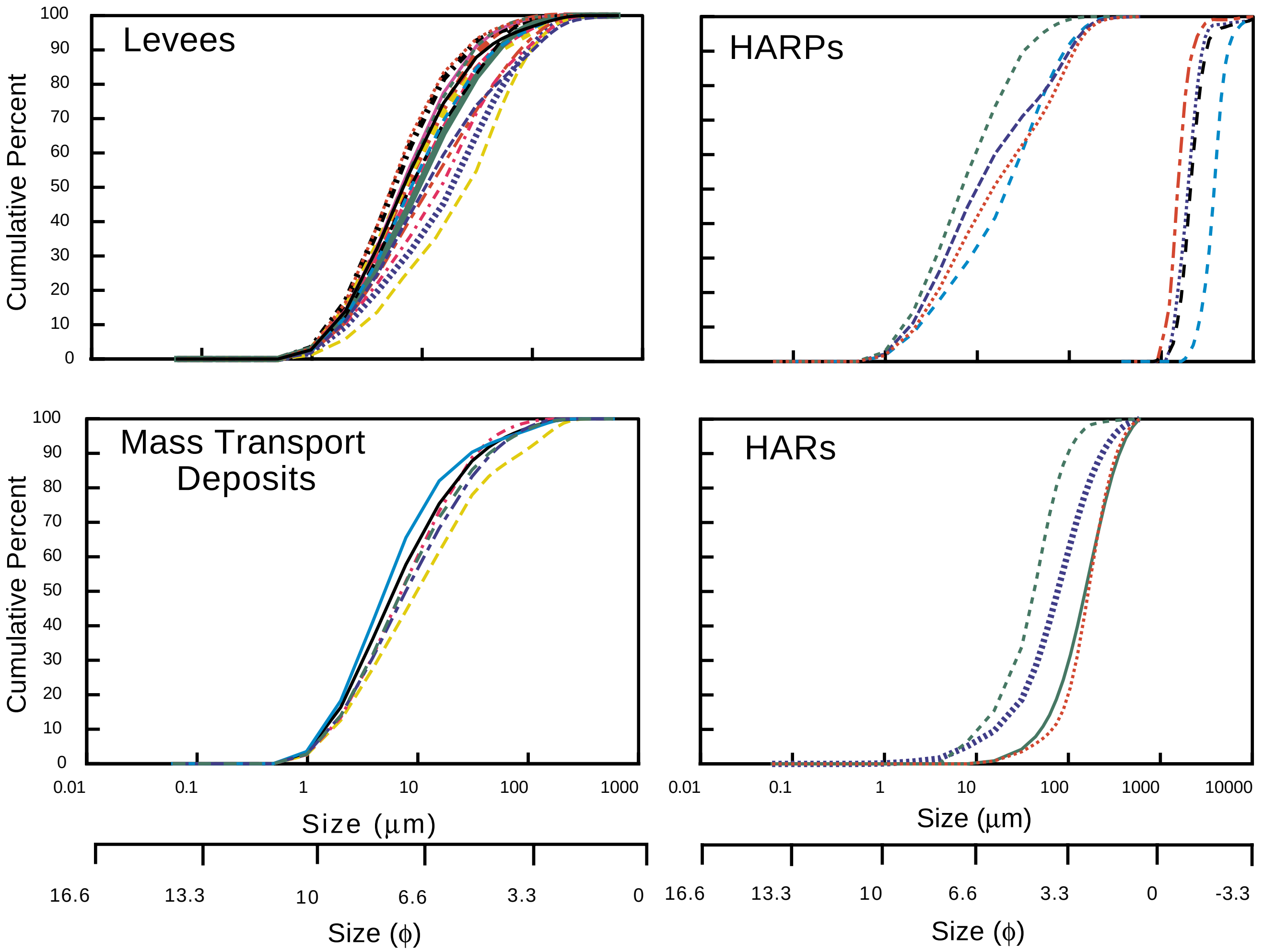

Figure 6. Typical cumulative frequency curves for the various architectural units found on the Amazon Fan. Levees and mass-transport deposits have similar grain-size distributions, whereas the HARP and the HAR units are the coarsest and best well-sorted material from the Amazon Fan.

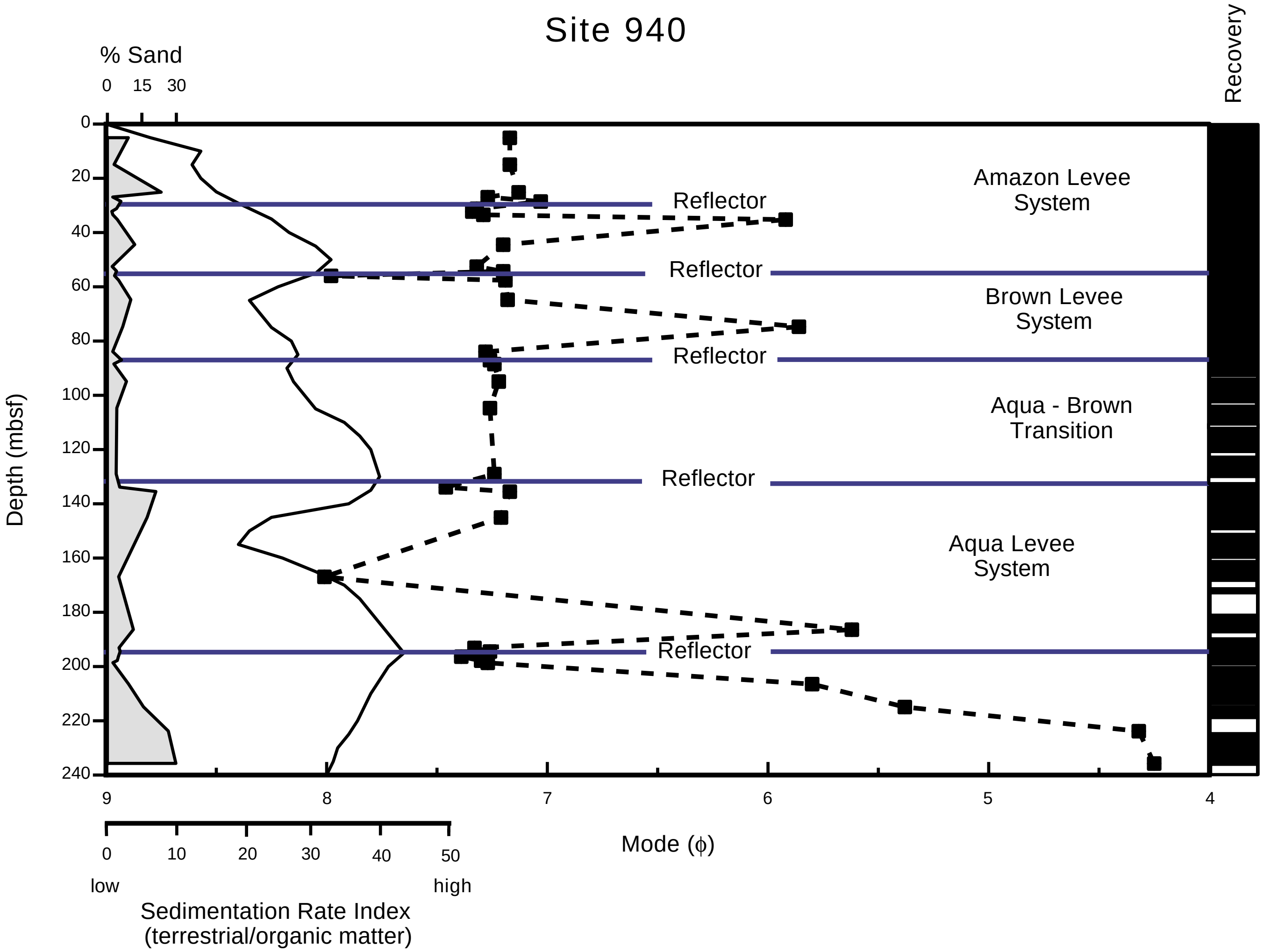

Figure 7. Downhole plot of mode size for individual sediment samples at Site 940. Key seismic reflectors associated with the bifurcation events of Aqua, Brown, and Amazon systems are superimposed on the grain-size data. The sedimentation rate index curve of Hinrichs and Rüllkötter (this volume) has been added for comparison as well as percent sand concentration downhole. Times of bifurcation appear to be related to higher sedimentation flux with an associated increase in coarser grained materials.

Channel, the last active channel on the fan, at the end of the last glacial period. They found a pattern of thinning and fining-upward of the turbidite sequences from the lower fan to the upper fan for the Amazon Channel-levee System. This trend was attributed to the slackening and/or shifting of the sediment source landward as the Amazon Channel received less sediment because the Amazon River debouched directly onto the continental shelf with the rising sea level. However, this study suggests that there is a general fining-upward trend for all channel levees. This includes levees found in all complexes and at all stages of fan development, not just at the end of a glacial cycle. Other factors must be contributing to this fining-upward trend.

Piper and Normark (1983) demonstrated that when a turbidity current is thick relative to the channel depth it can overtop the levee, stripping off the upper part of the flow and allowing the residual coarser portion of the flow to continue down channel. This process, termed "flow stripping," occurs when thick turbidity flows travel in channels having sharp bends. The characteristics of the sediments deposited on the levees are determined by complex interactions between the turbidity currents and the morphology of the channel. Individual turbidity currents evolve both through time and space, and so do the channel relief and slope, that in turn influence the flow conditions. Turbidity current overspill and the ensuing flux of sediment overbank will result whenever the flow is thicker than the height of the channel because flow turbulence and diffusion near the upper interface will tend to transport material from the channel to the surrounding clear water. A comprehensive set of field observations or numerical models does not yet exist to describe the spatial and temporal variations of turbidity currents in long sinuous channels. Numerical and experimental models (e.g., Parker et al., 1986; Stacey and Bowen, 1988; and references therein) do indicate that turbidity currents should become thicker as they travel downslope because of water entrainment from above. The resulting flow dilution tends to decrease the flow velocity, leading to sediment deposition and eventual dissipation of the turbidity current, unless the decrease in flow momentum is counteracted by other processes.

For turbidity currents confined to a channel, it is likely that the portion of the flow above the channel levees will spread laterally, possibly flowing down the steep levee flanks, becoming detached from the main flow in the channel (Pirmez, 1994; Hiscott et al., this volume). The upper portion of the flow carries the finer grained portion of the sediment load (Stacey and Bowen, 1988). Thus flow stripping provides a mechanism for grain-size sorting, with the finer material depositing in the levees and the coarser part of the load remain-

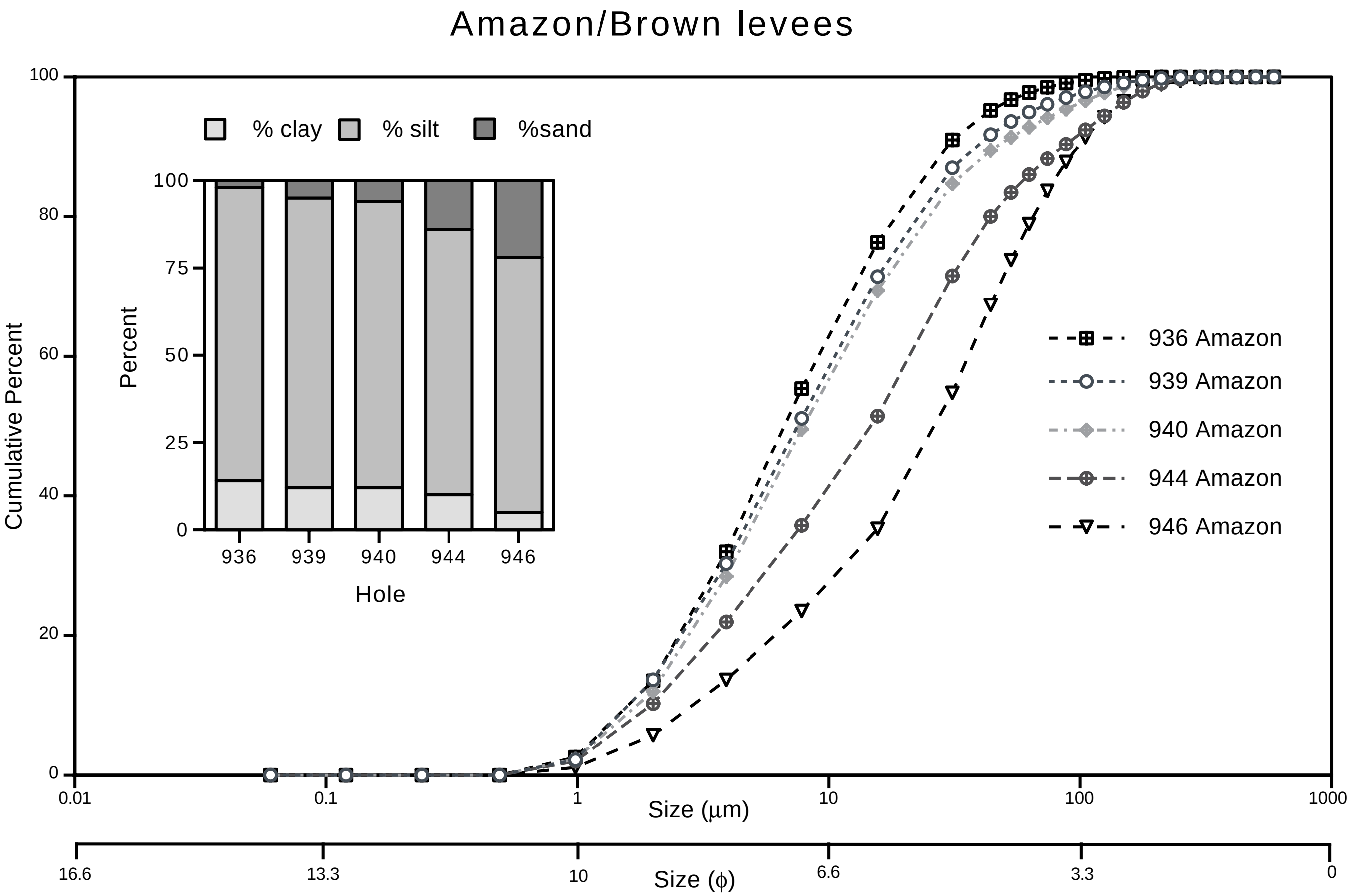

Figure 8. Averaged cumulative percent for the Amazon/Brown system for Sites 936, 939, 940, 944, and 946 provides a downfan trend for levee sediment deposition. There is a progressive shift to the right, indicating a downfan coarsening within the levee sediments. The inset histogram indicates the averaged sand-silt-clay percents for the five sites and demonstrates the increase in the percent of sand downfan.

ing in the channel. Flow density, and consequently velocity within the channel on the other hand, may increase if sediment is eroded from the channel floor and added to the turbidity current load. Denser, faster turbidity currents will also tend to become thinner, decreasing the potential to export sediment overbank (Piper and Normark, 1983). Turbidity currents traveling several hundreds of kilometers downfan must then continuously maintain a balance between flow thickening and dilution by entrainment, and increase in flow concentration by flow stripping and erosion. In addition, individual turbidity currents will be affected by spatial changes in channel sinuosity, slope, and cross-section. The grain-size sequence within the levees therefore contains a complex record of the interaction between flow and channel, and their changes through time.

The distinct fining-upward trend observed in all levee sequences is perhaps best explained by the overall increase in channel relief through time, which is clearly expressed in seismic reflection profiles across the channel levees (Manley and Flood, 1988; Pirmez, 1994; Pirmez and Flood, 1995). Soon after a bifurcation, the newly forming channel has little relief, and the lowermost portions of the turbidity current are allowed to spread laterally overbank (Fig. 3). With successive turbidity flows, levees begin to grow, increasing the channel relief. As the distance from flank crest to thalweg grows, progressively higher levels within the turbidity current will flow overbank, resulting in finer grain sizes being deposited on the levees. This is a continuous process, and the channel levees continue to grow in this manner until the next avulsion. Abandoned, the levee will only receive distal edges of proximal turbidity flows as well as some pelagic drape. Therefore, a channel levee should show a fining-upward trend as a response to its vertical growth in time and subsequent abandonment.

This simple cyclic response appears to explain the general fining-upward sequence observed on Amazon Fan levees, and is probably applicable to submarine fans in general. It is interesting to note that the fining-upward trend within the levee deposits is associated with general progradation of the levee system, that is, as the levee system grows vertically, it also advances both into deeper water as well as laterally. This general model provides a basis for interpreting the more complex records of grain-size trends observed where multiple levee growth phases are stacked upon each other upslope of bifurcation sites.

Vertical Grain-Size Cycles and Channel Bifurcations

Several fining-upward cycles are observed within channel levees at Sites 931, 936, 940, and 944. Site 940 sampled the levee deposits upslope of the Aqua bifurcation site (Figs. 1, 3). The levee deposits at this site record deposition from the onset of formation of the Aqua channel system to present day, including the Aqua to Brown, Brown to 1F and other younger bifurcations, until forming the youngest channel, Amazon Channel (Pirmez and Flood, 1995). Pirmez and Flood (1995), using acoustic stratal relationships, have demonstrated that after avulsion of a channel, there is an adjustment of the channel

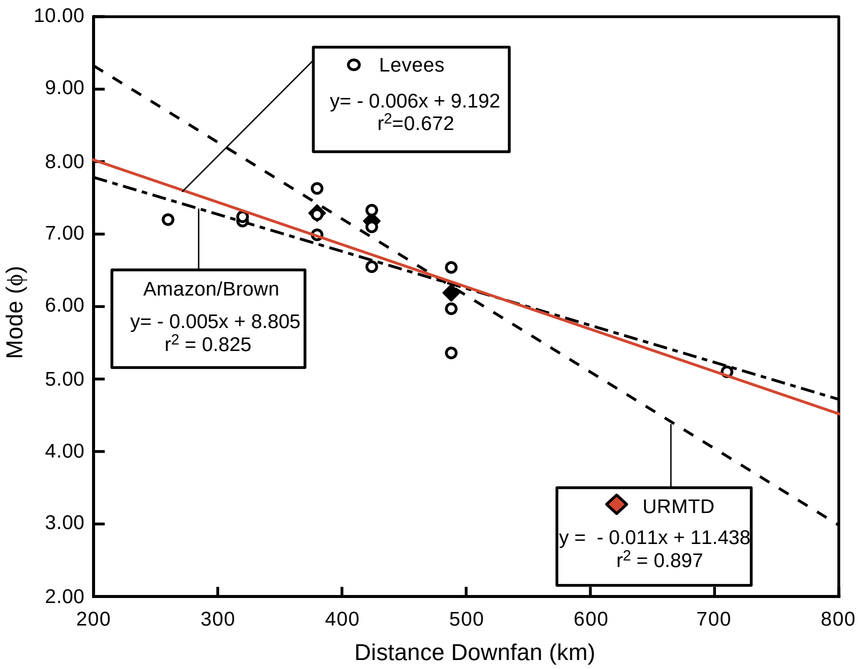

Figure 9. Average mode size of specified Amazon Fan units with distance downfan. Data includes channel levees sampled at locations having a downfan relationship with respect to each other. Linear regressions were computed for the Amazon/Brown levee site (same sites as in Fig. 8) as well as for levee data sampled at downfan sites. A downfan linear relationship also exits for samples within the URMTD.

profile with headward entrenchment and sediment bypass along with downfan aggradation. Using the measured thickness of channel and overbank deposits immediately upstream and downstream of a bifurcation points, the post-bifurcation deposits are thicker downfan of the bifurcation location. This rapid downfan aggradation, after an avulsion, is interpreted as indicating that channel bifurcations occur at periods of increased sediment discharge and channel progradation. As a result of a bifurcation, Pirmez and Flood (1995) state that thalweg entrenchment would rework older channel fill deposits and would cause an increase in the sand:mud ratio of the sediment load to the new pathway. This ratio would decrease with time as a new channel-levee system is established.

The stratal patterns observed within the levee deposits (Pirmez, 1994; Pirmez and Flood, 1995, fig. 18) show that the stacked alternation of levee progradational and aggradational units correlates closely to individual fining-upward cycles associated with each channel-levee growth phase. We have correlated abrupt changes in grain size with seismic reflectors corresponding to the avulsion events identified at Site 940 (Fig. 7). At key acoustic reflectors, which represent the base of the newly forming channel levee, there is a corresponding shift to coarser grained material. This is usually associated with a 5% to 15% increase in sand for the sediment samples analyzed near the depths of the avulsion reflectors. Independent estimates of sedimentation rate based on the ratio of terrestrial to marine organic matter (Hinrichs and Rüllkötter, this volume; also Fig. 7) suggest that there is an overall decrease in sedimentation rate through time over the whole levee column sampled at Site 940. Peaks in sedimentation rate index over 100× the index measured near the surface (linear sedimentation rate ~10 cm/ka) occur at the onset of the Brown and Amazon levee systems, and correspond closely to the trends observed in modal grain size. These observations support the premise that channel bifurcation is a result of increased influx (resulting from increased velocity, density, frequency) of turbidity currents introduced into the channel system, that is, they result from external controls (allocyclic) on the characteristics of turbidity currents.

An alternative hypothesis that cannot be entirely ruled out would be that the observed stacked depositional cycles within the levee deposits are autocyclic. They may be a result of periodic changes in channel relief or planform shape without invoking changes in the velocity and/or density of turbidity currents traveling through the channel. For instance, channel infilling by mass-transport deposits has been observed at Site 934 (Flood, Piper, Klaus, et al., 1995) as well as on other fans (e.g., Droz and Bellaiche, 1985). Rapid infilling of the channel and consequent decrease in channel relief should lead to coarsening of the overbank deposits, because lower levels in the ensuing turbidity currents will flow overbank.

Systematic changes in stratal characteristics (Pirmez and Flood, 1995) and grain-size trends are directly related to bifurcations at several sites along the Amazon Channel, and these avulsion events are characterized by a dramatic change in sediment type over broad regions downslope (e.g., thick sand-rich mass-flows or HARPs; Flood, Piper, Klaus, et al., 1995; also Pirmez et al., this volume). Thus it is difficult to explain the stacked fining-up sequences within the overbank deposits without invoking significant increases of turbidity current velocity or sediment flux (i.e. external controls, at the time of channel bifurcations).

The Amazon levee sampled at Sites 936 and 944 also shows several fining-upward cycles. These sites are located upslope of other bifurcation points along the Amazon Channel. Site 936 is located near the Brown bifurcation, whereas Site 944 is located near the 1F bifurcation (Pirmez and Flood, 1995). The observation of stacked fining-upward cycles at these three sites (Sites 940, 936, 944) indicates that channel bifurcations are directly related to changes in grain size within the levee deposits.

Spatial Changes of Levee Modal Grain Size

Sites 939, 940, 936, 944, and 946 sampled the Amazon/Brown channel, all located within 3 km of the levee crest, from the upper fan (Sites 939, 940), middle fan (Sites 936, 944) to the lower fan (Site 946). All sites are located on the eastern levee flank and are located in relatively straight reaches of the Amazon Channel. The exception is Site 936, which is located on the western levee flank on the outside bend of a meander of the Amazon Channel. An average cumulative percent was determined for the Amazon/Brown levee sediments at each site and indicates that there is a coarsening-downfan trend not only in mode size but in the relative ratio of clay:silt:sand (Fig. 8; Table 2). Using distance along the channel determined from high-resolution SeaBeam bathymetric survey of the Amazon Channel (Pirmez and Flood, 1995), a linear relationship between average phi mode size and distance downfan was determined (Fig. 9).

Though not sampled at as many sites, the Aqua (ULC), the Red (MLC), and the Green (LLC) levee systems were sampled at two separate locations allowing for downfan comparisons. The Aqua system (sampled at Sites 935 and 940, 60 km apart), the Red system (sampled at 936 and 944, 64 km apart), and the Green system (sampled at 935 and 944, 108 km apart) all show downfan coarsening. The linear correlation (Fig. 9) that exists between mode and distance downfan is more variable than that observed for the Amazon/Brown levee. This variability could be attributed to several factors such as imprecise distance determination along channel for the Red and Green channel systems and variable site distance away from the channel thalweg. While the Amazon/Brown levee locations were all within 3 km of the Amazon channel axis, one of the Red levee sites is 11 km away from the channel axis while the other site is within 3 km of the channel. In spite of local variations, the grain-size–downfan relationship within levee deposits shows a consistent downfan coarsening trend. Previous mapping of the complexes (Manley and Flood, 1988; Flood et al., 1991) showed that each levee complex developed from canyons positioned at different locations along the shelf break. The downfan coarsening trend in levee deposits, which is observed in three complexes, suggests that the control on grain-size trends is driven more by the dynamics of turbidity currents than by sediment source supply.

As previously stated, new channel levees form as a result of avulsion and grow vertically, probably because of a combination of flow stripping and fluid entrainment. This balance between channel relief and turbidity current thickness can also explain downfan coarsening trends observed in levees. As new levees grow in height, more of the turbidity flow is constrained within the channel. With time, the established channel levee slowly builds, channelizing more of the turbidity flow farther downfan. If flowstripping is a continuous process, the upper portion of turbidity current will be continuously removed and be deposited on the levees as it proceeds downfan, enriching the flow in coarser material. Because the distance between thalweg and levee crest decreases downfan (Pirmez and Flood, 1995), successive lower levels of the flow will be stripped away resulting in the observed downfan coarsening trend.

A similar trend of downfan coarsening was observed by Hiscott et al. (this volume) for turbidites recovered from the upper ~50 m of overbank deposits along the Amazon Channel. Though unable to correlate individual turbidite beds along the Amazon system, they find a strong correlation between median grain size and modern channel relief, supporting the idea that change in channel relief along the channel is the primary control on the grain size of the sediment that is deposited on the levees. Assuming that the samples taken at each site are representative of the different fan acoustic units, we find that the same downfan coarsening trends occur in all channel-levee systems drilled on the Amazon Fan.

HARs and HARPs

HARs beneath the channel axis (Kastens and Shor, 1986; Stelting et al., 1985) and HARPs beneath levee deposits (Flood et al., 1991) comprise the acoustic facies yielding the coarsest sediment yet retrieved from the Amazon Fan. These units had generally poor core recovery, and the HARPs in particular are characterized in more detail through logging and core data elsewhere (Pirmez et al., this volume).

HARs have been associated with the axis of channel-levee systems on most submarine fans, and were originally thought to be lag deposits in the channel thalweg. Yet other work has suggested that at least part of the reflective nature of HARs may be an acoustic artifact caused by side echoes off a sinuous channel (Flood, 1987). The upper portion of a HAR was sampled on the Mississippi Fan (Leg 96) and found to contain coarse gravel (Bouma, Coleman, Meyer, et al., 1986).

The HAR unit associated with the Amazon Channel was sampled at three sites (Sites 943, 945, and 934 at a cut-off meander loop). These sediments are the coarsest and best-sorted material sampled within the Amazon deep-sea fan and represent the channel sands that are moved down the fan with each successive turbidity current (Fig. 6). Based on grain-size analyses from Sites 943 and 945, the HAR unit is composed of alternating finer and coarser grained sediments that are well sorted (Figs. 4, 5). At Site 943, the two distinct grain-size populations have modes of 2.6 ø (coarse-grained sediment) and 4.4 ø (fine-grained sediment) with clay:silt:sand ratios of 0:9:91 and 0:72:28, respectively. By Site 945, 220 km downfan from Site 943, the HAR still has two distinct, well-sorted grain-size populations. The coarser mode (2.4 ø, 0:14:86) is similar to that determined at Site 943; however, the finer mode (3.4 ø, 1:41:58) has coarsened downfan by 1 ø. The coarsening downfan of the medium sand fraction indicates that the turbidity currents are still effectively sorting this size range. However, the coarsening trend is inconsistent with deposition from the same flows, as there is a general decrease in slope, and presumably current velocity decreases downfan. Sediment reworking during multiple phases of channel bifurcation is probably the cause of downfan coarsening. The constant size for the fine-sand fraction may be an indicator of the maximum size that can be transported downfan given the distance and gradient of the fan, or it may be the maximum size available in the system.

High-amplitude reflection packets (HARPs) have been identified to be associated with channel bifurcations (Flood et al., 1991) and are thought to represent the flows that begin when an avulsion event breaches a channel levee (Fig. 3). The coarser, unchannelized deposits accumulate downslope from the newly forming channel mouth as the channel grows downfan. The HARP unit associated with the Amazon levee and its associated channel bifurcations were sampled at three locations (Sites 935, 936, 944). Similar to the HARs, HARPs have two distinct grain-size populations (Figs. 4, 6). At Site 935 the two populations have modes that are 7.4 ø (14:83:3) and 1.1 ø (0:1:99). Downfan at Site 936, the finer sediments have a mode of 7.6 ϕ (14:80:6), whereas the coarser fraction is 2.7 ø (0:14:86). At Site 944 only one population was recovered and had an intermediate modal value of 5.2 ø (8:74:18).

Considering the finer fractions for each site, they are only slightly coarser than the overlying Amazon channel levee. The coarser fractions sampled at Sites 935 and 936 are within the range of the grain sizes determined within the HAR unit sampled at Site 943 (only 66 km downfan from Site 936). The grain-size data support the idea that the HARP units are reworked channel levees and channel lag deposits. The bimodality of samples and downfan changes observed in these sand-rich units probably result from stacking of multiple bifurcation events. For instance, at Sites 935 and 936, the HARP units resulting from the Aqua bifurcation are superposed onto older distal levee deposits of the Aqua and older systems, including sand-rich units probably associated with older channel systems. More detailed sampling, guided by seismic and logging data studies (e.g., Pirmez et al., this volume) will be required to refine spatial changes in grain size within this unit.

Mass-Transport Deposits

Three large mass-transport deposits were sampled during Leg 155. Although discussed by Piper et al. (Chapter 6, this volume) in more detail, the grain size was determined on each of these units. The Western Debris Flow (WMTD at Site 941; Piper et al., Chapter 6, this volume) has a slight coarsening-upward trend (Fig. 4). The WMTD (average mode, 7.9 ø) is finer than URMTD at either Site 935 (7 ø, 15:79:6) or Site 936 (7.2 ø, 14:83:3) and the BMTD found at Sites 931 (7.1 ø, 13:80:7) and 933 (6.9 ø, 14:79:7) (Table 2).

URMTD was first recognized on seismic profiles as an acoustically transparent deposit (devoid of any high-amplitude reflectors) that filled in topographic lows and separated the ULC from the LLC. This acoustic unit was inferred to be the result of one or more slump/debris flow deposits (Manley and Flood, 1988), which was confirmed by drilling at Sites 935, 936, and 944 (Flood, Piper, Klaus, et al., 1995). However, its aerial distribution was found to be smaller than previously estimated (Piper et al., Chapter 6, this volume).

Sites 935, 936, and 944 span approximately 100 km downfan. At Site 935, the clay:silt:sand ratio is 15:79:6 with a mean mode size of 7.1 ø. Approximately 35 km downfan at Site 936 the clay:silt:sand ratio has changed slightly to 13:84:3 with nearly the same mode 7.2 ø. By Site 944 (64 km farther downfan), the clay:silt:sand ratio is 11:68:21 and the average mode is 5.8 ø (Fig. 4; Table 2). URMTD is 0.2–0.5 ø coarser than the Amazon levee at Sites 935 and 944, whereas its nearly identical to the Amazon levee at Site 936. There is a coarsening downfan trend, and a first order linear relationship between distance downfan and grain size for URMTD can be made (Fig. 9). Since Site 944 is within 22 km of the downfan terminus of the URTMD, this site may have sampled the distal edge of the deposit, which may be anomalously coarse, resulting in the downfan coarsening trend observed. This seems consistent with the downhole mode trends. URMTD shows an overall fining-upward sequence that has similar clay:silt:sand ratios to those of the channel levees located stratigraphically above or below it at Sites 935 and 936 (Table 2). Yet at Site 944 the mode appears to have a coarsening upward trend within the lower section of the deposit but is 2 ø finer in the upper 15 m of the unit.

Originally thought to be part of Unit R, a buried debris-flow unit (BMTD of Piper et al.,Chapter 6, this volume) was sampled at Sites 931 and 933. The average mode size of the BMTD is 6.9 ø with a clay:silt:sand ratio of 14:79:6 at Site 933, and 7.1 ø with a clay:silt:sand ratio of 13:80:7 for Site 931, which is slightly downfan from Site 933. At Site 933, the BMTD fines upward but at Site 931 it appears to have a slight coarsening-upward trend. At Site 933, the BMTD can be subdivided at 125 mbsf based on grain size. The lower unit is coarser than the upper unit. The BMTD is slightly coarser than channel levees sampled at each site and has a comparable mode size and clay:silt:sand ratio as URMTD at Sites 935 and 936.

SUMMARY AND CONCLUSIONS

1. All channel levees sampled display a fining-upward sequence and an overall coarsening downfan. These grain-size trends are the result of sediment sorting within a channel that decreases in relief in the downfan direction and that grows in relief through time.

2. Stacked fining-upward sequences within levee deposits result from cyclic bifurcation of the channel downslope from a site. An abrupt coarsening at the base of individual levee sequences probably correspond to an increase in sediment flux, caused by one or more factors such as an increase in velocity, density or thickness of turbidity currents.

3. Mass-transport deposits generally show a fining-upward sequence with a coarsening downfan, with characteristics similar to the trends observed in levee deposits. Only two sites, Site 931 sampling the BMTD, and Site 941 sampling the WMTD, showed a slight coarsening-upward trend. Grain size of the debris flows is slightly coarser than the channel-levee deposits.

4. Both channel-lag deposits (HAR facies) and mass-flows at the base of levee deposits (HARP facies) are well sorted and are composed of two different grain-size sediment layers. Both units show a downfan coarsening for the finer fraction but a more consistent grain size for the larger fraction. Downfan coarsening probably results from the stacking of multiple sediment transport events associated with channel bifurcations.

Our conclusions based on grain-size trends imply that the dynamics within a turbidity current respond to an overall change in channel-relief growth both vertically and downfan. The overall fining-up trends in all levee deposits would indicate that the interaction of turbidity currents and channel morphology probably is the primary control in the grain size of overbank deposits, a conclusion also reached by Hiscott et al. (this volume).Variations from this grain-size trend certainly occur, as observed when multiple phases of levee growth are stacked within a levee deposit. Here several processes, including changes in channel morphology associated with the avulsion process (levee aggradation, entrenchment, infilling) (Pirmez and Flood, 1995), as well as external forcing such as sea-level changes, climate variability, or local switching of the Amazon River mouth, certainly influence the grain size of the sediment transported by turbidity currents and deposited overbank. We propose that the systematic occurrence of stacked fining-up sequences, separated by abrupt coarsening at the base associated with widespread deposition of sand-rich mass-flows downfan, record marked increases in the flux of sediment transported by turbidity currents into the fan. Thus the general fining-upward trend can be modulated by changes in the flow characteristics at times of bifurcations generating the stacked cyclic patterns. How exactly the grain-size load of turbidity currents responds as the characteristics of individual flows change in response to sea-level changes, climate variability, or switching of the Amazon River mouth is not addressed here. However, since each levee complex appears to form during a major sea-level lowstand (~100 ka), and individual levee systems appear to bifurcate at short time intervals of the order of 1 to 10 ka, forcing mechanisms would have to act over very high frequency to explain the grain-size record within the channel-levee systems.

ACKNOWLEDGMENTS

Financial support for the processing and analysis of the data used in this study was provided by JOI/USSSP. We thank Dr. Eugene Domack for the use of Hamilton College's Malvern MasterSizer E for the grain-size analysis. We wish to acknowledge the technical support of Sarah E. Lee, Happy Hazelton, Meredith Frinsko, and Laura Manley for the grain-size analyses. The authors wish to thank Ben Kneller and Suzanne O'Connell for their helpful reviews of a previous manuscript.

REFERENCES

Appi, C.J., Kowsmann, R.O., Flood, R.D., Manley, P.L., and Pirmez, C., 1988. Evoluçao Quaternária Pós-Glacial do cone submarino do Amazonas: um modelo retrogradante. *Avais XXXV Congr. Brasileriro Geol.*, 2:451–465.

Bouma, A.H., Coleman, J.M., Meyer, A.W., et al., 1986. *Init Repts. DSDP*, 96: Washington (U.S. Govt. Printing Office).

Damuth, J.E., and Embley, R.W., 1981. Mass-transport processes on the Amazon Cone: western equatorial Atlantic. *AAPG Bull.*, 65:629–643.

Damuth, J.E., and Flood, R.D., 1984. Morphology, sedimentation processes, and growth pattern on the Amazon deep-sea fan. *Geo-Mar. Lett.*, 3:109–117.

Damuth, J.E., Flood, R.D., Kowsmann, R.O., Belderson, R.H., and Gorini, M.A., 1988. Anatomy and growth pattern of Amazon deep-sea fan as revealed by long-range side-scan sonar (GLORIA) and high-resolution seismic studies. *AAPG Bull.*, 72:885–911.

Damuth, J.E., Kolla, V., Flood, R.D., Kowsmann, R.O., Monteiro, M.C., Gorini, M.A., Palma, J.J.C., and Belderson, R.H., 1983a. Distributary channel meandering and bifurcation patterns on Amazon deep-sea fan as revealed by long-range side-scan sonar (GLORIA). *Geology*, 11:94–98.

Damuth, J.E., Kowsmann, R.O., Flood, R.D., Belderson, R.H., and Gorini, M.A., 1983b. Age relationships of distributary channels on Amazon deep-sea fan: implications for fan growth pattern. *Geology*, 11:470–473.

Droz, L., and Bellaiche, G., 1985. Rhône deep-sea fan: morphostructure and growth pattern. *AAPG Bull.*, 69:460–479.

Flood, R.D., 1987. Side echoes from a sinuous fan channel obscure the structure of submarine fan channel/levee systems, Amazon fan. *Geo-Mar. Lett.*, 7:15–22.

Flood, R.D., Manley, P.L., Kowsmann, R.O., Appi, C.J., and Pirmez, C., 1991. Seismic facies and late Quaternary growth of Amazon submarine fan. *In* Weimer, P., and Link, M.H. (Eds.), *Seismic Facies and Sedimen-*

tary Processes of Submarine Fans and Turbidite Systems: New York (Springer), 415–433.

Flood, R.D., Piper, D.J.W., Klaus, A., et al., 1995. *Proc. ODP, Init. Repts.*, 155: College Station, TX (Ocean Drilling Program).

Gibbs, R.J., Matthews, M.D., and Link, D.A., 1971. The relationship between sphere size and settling velocity. *J. Sediment. Petrol.,* 41:7–18.

Kastens, K.A., and Shor, A.N., 1985. Depositional processes of a meandering channel on Mississippi Fan. *AAPG Bull.,* 69:190–202.

Manley, P.L., and Flood, R.D., 1988. Cyclic sediment deposition within Amazon deep-sea fan. *AAPG Bull.,* 72:912–925.

McCave, I.N., Bryant, R.J., Cook, H.F., and Coughanowr, C.A., 1986. Evaluation of a laser-diffraction-size analyzer for use with natural sediments. *J. Sediment. Petrol.,* 56:561–564.

Parker, G., Fukushima, Y., and Pantin, H.M., 1986. Self-accelerating turbidity currents. *J. Fluid Mech.,* 171:145–181.

Piper, D.J.W., and Normark, W.R., 1983. Turbidite depositional patterns and flow characteristics, Navy Submarine Fan, California Borderland. *Sedimentology,* 30:681–694.

Pirmez, C., 1994. Growth of a submarine meandering channel-levee system on the Amazon Fan [Ph.D. thesis]. Columbia Univ., New York.

Pirmez, C., and Flood, R.D., 1995. Morphology and structure of Amazon Channel. *In* Flood, R.D., Piper, D.J.W., Klaus, A., et al., *Proc. ODP, Init. Repts.,* 155: College Station, TX (Ocean Drilling Program), 23–45.

Posamentier, H.W., Erskine, R.D., and Mitchum, R.M., Jr., 1991. Models for submarine fan deposition within a sequence-stratigraphic framework. *In* Weimer, P., and Link, M.H. (Eds.), *Seismic Facies and Sedimentary Processes of Submarine Fans and Turbidite Systems:* New York (Springer), 127–136.

Posamentier, H.W., and Vail, P.R., 1988. Eustatic controls on clastic deposition, II: Sequence and systems tract models. *In* Wilgus, C.K., Hastings, B.S., Ross, C.A., Posamentier, H.W., Van Wagoner, J., and Kendall, C.G.St.C. (Eds.), *Sea-Level Changes: An Integrated Approach.* Spec. Publ.—Soc. Econ. Paleontol. Mineral., 42:125–154.

Stacey, M.W., and Bowen, A.J., 1988. The vertical structure of density and turbidity currents: theory and observations. *J. Geophys. Res.,* 93:3528–3542.

Stelting, C.E., Pickering, K.T., Bouma, A.H., Coleman, J.M., Cremer, M., Droz, L., Meyer-Wright, A.A., Normark, W.R., O'Connell, S., Stow, D.A.V., and DSDP Leg 96 Shipboard Scientists, 1985. Drilling results on the middle Mississippi fan. *In* Bouma, A.H., Normark, W.R., and Barnes, N.E. (Eds.), *Submarine Fans and Related Turbidite Systems:* New York (Springer), 275–282.

Stow, D.A.V., Cremer, M., Droz, L., Normark, W.R., O'Connell, S., Pickering, K.T., Stelting, C.E., Meyer-Wright, A.W., and DSDP Leg 96 Shipboard Scientists, 1985. Mississippi Fan sedimentary facies, composition, and texture. *In* Bouma, A.H., Normark, W.R., and Barnes, N.E. (Eds.), *Submarine Fan and Related Turbidite System:* New York (Springer-Verlag), 259–266.

Stow, D.A.V., and Wetzel, A., 1990. Hemiturbidite: a new type of deep-water sediment. *In* Cochran, J.R., Stow, D.A.V., et al., *Proc. ODP, Sci. Results,* 116: College Station, TX (Ocean Drilling Program), 25–34.

Date of initial receipt: 5 December 1995
Date of acceptance: 3 May 1996
Ms 155SR-209